Physics – Uspekhi **60** (10) 994 – 1017 (2017)

REVIEWS OF TOPICAL PROBLEMS PACS numbers: 28.41.Kw, 52.25.Xz, **52.30.–q**, **52.75.–d**

Separation of mixtures of chemical elements in plasma

D A Dolgolenko, Yu A Muromkin

DOI: https://doi.org/10.3367/UFNe.2016.12.038016

Contents

Abstract. This paper reviews proposals on the plasma processing of radioactive waste (RW) and spent nuclear fuel (SNF). The chemical processing of SNF based on the extraction of its components from water solutions is rather expensive and produces new waste. The paper considers experimental research on plasma separation of mixtures of chemical elements and isotopes, whose results can help evaluate the plasma methods of RW and SNF reprocessing. The analysis identifies the difference between ionization levels of RW and SNF components at their transition to the plasma phase as a reason why all plasma methods are difficult to apply.

Keywords: plasma centrifuge, magnetic trap, centrifugal trap, ion cyclotron resonance, spent nuclear fuel

1. Introduction

Mixtures of chemical elements are, as a rule, separated by chemical means. The same refers to processing the radioactive waste (RW) and spent nuclear fuel (SNF). However, the method for chemical reprocessing of RW and SNF aqueous solutions has the important disadvantage of producing large amounts of liquid radioactive waste. This is especially true of the main reprocessing procedure, i.e., plutonium–uranium recovery by extraction (PUREX). Therefore, as early as the 1950s, chemists initiated research directed toward developing a 'dry' fluoride volatility method for RW and SNF processing [1–3]. However, this technique has not yet found application in industry.

In the 1990s, researchers in the USA began experimenting with ways to eliminate by physical means one of the problems pertinent to RW storage. Archimedes Technology Group Inc. (ATG) announced its intention to undertook accelerated reprocessing of liquid radioactive waste from plutonium production (the result of partial reprocessing of irradiated uranium) at the Hanford site. By that time, the waste storage tanks had been outworn due to corrosion. In that RW [4], 99.9% of the radioactivity came from atoms with mass above 89 a.m.u., but their processing was inefficient. Specifically, atoms weighting less than 60 a.m.u. accounted for 82% of the mass immobilized in a glassy matrix to be buried.

ATG set the goal to separate the radioactive fraction of the waste from ballast products in an attempt to reduce several-fold the mass of RW to be buried. The project envisaged processing tens of thousands of tons of the then-accumulated RW [5]. For this purpose, the mass separation effect of rotating plasma predicted by Ohkawa [6] was employed with the use of a separation device termed a *plasma mass filter*, hereinafter referred to as the Archimedes plasma mass filter (APMF) (see report [5] where this abbreviation

D A Dolgolenko, Yu A Muromkin
National Research Centre 'Kurchatov Institute',
pl. Akademika Kurchatova 1, 123182 Moscow, Russian Federation
E-mail: dolgolenko_da@nrcki.ru, muromkin_ya@nrcki.ru

Received 18 October 2016, revised 9 December 2016
Uspekhi Fizicheskikh Nauk **187** (10) 1071 – 1096 (2017)
DOI: https://doi.org/10.3367/UFNr.2016.12.038016
Translated by Yu V Morozov; edited by A Radzig

was introduced). In a plasma centrifuge of conventional geometry with crossed electric and magnetic fields and electric drift velocity $\mathbf{v}_E = c[\mathbf{EH}]/H^2$, such an effect is possible only if a force acting on ions in the radial electric field has the same direction as the centrifugal force, i.e., if a positive electric potential is applied to the central electrode. It was calculated that at the plasma rotation rate $\omega_E \approx \omega_{ci}/2$ in crossed fields, where $\omega_{ci} = eH/(M_i^c c)$ is the cyclotron frequency of an ion with mass M_i^c (cut-off mass [5]), ions having mass $M_i > M_i^c$ fail to be confined in the plasma volume and escape onto the walls of the discharge chamber. The effect ideally conformed to the requirements for disposal of the radioactive components of the waste. By varying the strengths of the electric and magnetic fields, it was possible to arrive at the M_i^c value needed for the purpose. Putting this effect into practice promised the possibility of achieving the goal set by ATG with the use of a plasma single-pass separator.

A tandem plasma mass filter [7] was chosen to implement the ATG project. In this device, the mixture undergoing separation was fed into the center of the discharge chamber and its heavy fraction was disposed of the same place, whereas light fractions were removed at both ends of the chamber. ATG built up a large demonstration facility (Demo). Preliminary results of Demo experiments were reported at the conference [5]. Another publication concerning RW ionization discussed model experiments with argon ionization by helicons (circularly polarized waves) excitable at a frequency of 6 MHz) [8]. A detailed description of the method with excellent illustrations could be found on the ATG website. The work carried out by ATG was highlighted at the 30th European Physical Society Conference on Controlled Fusion and Plasma Physics held in St. Petersburg in 2005 [5]. The results thus obtained became widely known in Russia.

It should be emphasized that the effect on which the separation technique being considered is based has never before been observed in experiment. This was attributed in Ref. [6] to the fact that a negative potential was applied to the central electrode in experiments with plasma centrifuges. To recall, the negative potential at the central electrode was usually maintained in stationary plasma centrifuges to ensure stable emission of electrons from the cathode. Also, pulsed plasma centrifuges were used in experiments with a positive potential at the central electrode [9–11]. It was argued that a *collisionless* rotating plasma is needed for the APMF to function [4, 5]. As a rule, no experiments with plasma centrifuges were conducted under such conditions. Reference [12] reported experiments with the reflective (Penning) discharge in a low-density plasma in which the separation effect, i.e., selective escape of resonant ions along the magnetic lines at $\omega_E \approx \omega_{ci}/2$, was observed. The authors of this study attributed the ion heating and removal to the development of resonant ion cyclotron instability (ICI). This effect was not mentioned in publications [4, 5].

Information about further ATG activities has become unavailable since 2006. The shutdown was never reported officially, but it appeared obvious with time.

In the early 2000s, researchers at the National Research Centre (NRC) 'Kurchatov Institute' proposed to process RW and SNF using the plasma-optical method (Morozov et al. [13]) and ion cyclotron resonance (ICR) in plasma (Smirnov et al. [14, 15]). Soon after that, research in this field was initiated at the NRC Kharkiv Institute of Physics and Technology, Ukraine, by Egorov, Skibenko, Yuferov, and co-workers [16–18].

The problem of processing RW and SNF has of necessity emerged once again in connection with the Fukushima nuclear disaster in Japan (11 March 2011). It induced Fetterman and Fisch of the Princeton Plasma Physics Laboratory (PPPL), USA, to resort to plasma-based processes for RW and SNF treatment [19, 20].

The present review deals with the known experimental research on plasma separation of the mixtures of chemical elements and isotopes, the results of which can help evaluate the applicability and efficiency of plasma-based reprocessing techniques. We discuss the physical principles underlying the separation process in a manner enabling professional chemists to comprehend the essence of the proposed approach with only passing reference to purely technical issues.

We believe it expedient to begin the review of plasma technologies from separation of the mixtures of chemical elements with the use of plasma centrifuges (Section 2). To-day, certain authors link the success of RW and SNF processing with the exploitation of rotating plasma. These proposals, starting with APMF, are considered in Sections 3–5. At the time of keen interest in plasma centrifuges, they were not intended for this purpose; rather, they were used largely to separate isotopes. But one modification proposed by Krishnan, Geva, and Hirshfield of Yale University [21] is worth mentioning in greater detail. Experiments with this device, designed to develop a new method for isotope separation, actually launched the beginning of RW/SNF reprocessing research and the creation of its simplest model. In those studies, the authors used cathodes fabricated from binary alloys and evaluated separation efficiency from sediment composition formed by the plasma stream at the exit from the centrifuge [21, 22]. They showed that separation of chemical elements in a plasma centrifuge does not always occur as isotope separation does due to the difference in ion masses and charges for separable components. Specifically, the light component of the Al–Ti mixture proved to be in equilibrium at the periphery of the centrifuge rather than on its axis. Such a centrifuge, called a *vacuum-arc centrifuge* (VAC) [22], is chiefly considered in Section 2. There is no generally accepted exact equivalent to this term in Russian, because it implies an arc in the vapors released from the surface of electrodes in a vacuum. Such arcs are known to sometimes appear for a very short time in vacuum switches [23].

There are detailed reviews of publications concerning plasma isotope separation by different methods, including the use of plasma centrifuges (see, for instance, reviews [24, 25]). References [26, 27] are specially devoted to plasma centrifuges. These reviews present results of research carried out before the late 1980s. The paper by Whichello, Evans, and Simpson [28] reflects the state-of-the-art in VAC technology as of 1994. Our review includes as well later studies designed to enhance the separation power of VACs. Of special interest is the recent proposal to create a VAC cascade [29], bearing in mind the impossibility of one-step isotope separation. The idea of plasma centrifuge isotope separation by a cascade of processes was especially popular in the early period of research with reference to ^{48}Ca, ^{203}Tl, ^{68}Zn separation [30]. On the other hand, cascading is utterly undesirable as far as RW and SNF reprocessing by plasma technologies is concerned, because it implies repeated manipulation of radioactive substances.

Section 3 deals with the Archimedes plasma mass filter proposed by Ohkawa [6] in the late 1990s and extensively explored by ATG.

Section 4 reviews investigations carried out to develop a method for SNF processing at the NRC Kharkiv Institute of Physics and Technology. The authors of Ref. [16] consider a variety of plasma-based separation methods under the umbrella term *magnetoplasma separation techniques* used here only as the title for Section 4.

Section 5 is designed to discuss the proposal by Fetterman and Fisch [19, 20] to fabricate an asymmetric centrifugal trap to process RW and SNF and call the relevant device a *magnetic centrifugal mass filter* (MCMF).

The centrifugal trap (CT) differs from the magnetic mirror trap in that it exploits the second (centrifugal) mechanism for plasma confinement. The plasma in a CT is driven into rotation, which facilitates its confinement [31], because the distance between the magnetized charged particles and the trap axis decreases as they approach the magnetic mirror along magnetic lines of force, while the rotation rate increases due to angular momentum conservation.

It is maintained that, in a trap with one mirror being primarily magnetic and the other largely centrifugal [the so-called *asymmetric centrifugal trap* (ACT)], the choice of the proper mirror-to-mirror ratio creates conditions under which heavy ions escape through the magnetic mirror and light ones through the centrifugal plug. The advantage of utilizing an ACT in a neutronless thermonuclear reactor (based on the $p + {}^{11}B \rightarrow 3\,{}^{4}He + 8.7$ MeV reaction) was pointed out by Volosov [32, 33], who believed it possible to create conditions under which main plasma particles and thermonuclear reaction products ('ash') escape from the opposite mirrors. Fetterman and Fisch proposed, with reference to paper [32], to apply ACT for separation in cold plasma.

Section 6 is focused on plasma-optical mass separation (POMS). The ultimate objective of one of the variants of this technology (POMS proper) is the development of a separator of the same quality as the electromagnetic (EM) one [34, 35] but several orders of magnitude superior to it in terms of productive capacity [36]. Naturally, such a separator could also be employed to process RW and SNF [37]. Section 6 contains a description of some other plasma-based separation techniques [38–40] without their being stringently classified as plasma-optical [41].

Section 7 is primarily concerned with the application of ion cyclotron resonance for plasma-based processing of RW and SNF. This method was theoretically substantiated by A V Timofeev, who summarized results of the work in a recent review [42]; therefore, we confine ourselves to the concise characteristics of this technique. The available experimental data have thus far come only from ICR separation of isotopes. In fact, the sole known experiment on ICR separation in a mixture of chemical elements resulted in the recovery of gold from an Au–Cu–Zn alloy [43].

The concluding Section 8 contains our notes as regards evaluation of the productive capacity of the described plasma technologies for separation of RW and SNF components.

2. Plasma centrifuge

2.1 History

According to a widely-held opinion, the main advantages of plasma centrifuges include the simple mechanical design (the absence of moving parts) and the high rotation velocity (one or two orders of magnitude greater than the rotor rotation rate in gas centrifuges).

Plasma centrifuges first attracted the attention of researchers in the USA as devices suitable for uranium isotope separation in the course of implementation of the Manhattan Project, but the first experiments proved to be a failure [44]. The next stage of research began after the Swedish physicist B Bonnevier had theoretically demonstrated in 1966 the possibility of applying magnetic hydrodynamics for ion mass separation in a fully ionized dense plasma rotating in crossed electric and magnetic fields [45]. In 1971, Bonnevier reported the first experiments with a pulsed plasma centrifuge [46] used to successfully separate hydrogen and neon isotopes (paper [46] also included the results of the preceding theoretical work [45]). Even if the author failed to obtain a fully ionized plasma, his research gave an impetus to numerous experimental studies on plasma centrifuges.

B Lehnert, another Swedish researcher [47], suggested that a partially ionized plasma can be employed to separate isotopes on the assumption that it combines a high rotation rate and relatively low plasma temperature; moreover, isotope separation efficiency of a plasma centrifuge can be estimated using the known formula for gas centrifuges [48] in which the separation factor of a binary mixture is given by

$$\alpha = \frac{(c_1/c_2)_{\mathrm{r}}}{(c_1/c_2)_0} \propto \exp\left(\frac{\Delta M \omega^2 r^2}{k_{\mathrm{B}} T}\right).$$

Here, $(c_1/c_2)_{\mathrm{r}}$ and $(c_1/c_2)_0$ are the ratios between concentrations of components in the binary mixture at the periphery and on the axis of the centrifuge, respectively, ΔM is the difference between masses, ω is the rotation rate, T is the temperature, r is the centrifuge radius, and k_{B} is the Boltzmann constant.

The results of the separation process are usually characterized by the achieved separation factor α. In studies on new separation methods, this coefficient is normally calculated by comparing concentrations of the isotope (or the chemical element) to be extracted at the output (product) and in the supplying stream. Normally, the concentration of an isotope in the supplying stream corresponds to its natural concentration. The quantity

$$\alpha = \frac{c_{\mathrm{p}}(1 - c_0)}{c_0(1 - c_{\mathrm{p}})},$$

where c_{p} is the concentration of the isotope of interest in the product, and c_0 is its concentration in the supplying stream. This formula is valid for a binary mixture. For multicomponent mixtures, quantities $1 - c_0$ and $1 - c_{\mathrm{p}}$ denote the total concentration of all the remaining components. The concentration of a given isotope (or a chemical element) in the waste, c_{w}, is used to calculate the plasma stream depletion factor $\beta = [c_{\mathrm{w}}(1 - c_0)]/[c_0(1 - c_{\mathrm{w}})]$.

The efficiency of extraction is characterized by extraction factor γ defined as the ratio of the amount of a given component of the mixture deposited on the collector to that transferred by the plasma stream for the same time.

The application of a gas discharge in crossed electric and magnetic fields in a neutral gas (neon isotopes) to achieve separation effect is exemplified by experiments carried out by James and Simpson (University of Sydney, Australia) [49], in which the separation effect showed itself in inertially rotating neon following a short-term discharge. Experiments with

pulsed plasma centrifuges and partially ionized plasma were carried out in two laboratories at NRC 'Kurchatov Institute', Moscow. The laboratory headed by A I Karchevskii studied centrifuge characteristics based on the results of separation of inert gas isotopes and their mixtures [10, 11]. The objective of the work was, in particular, to develop a highly efficient method for separating isotopes of alkaline and alkali-earth elements normally separated with the use of low-efficiency EM separators. The other laboratory headed by V D Rusanov planned to design a plasma centrifuge-based plasmachemical reactor [50]. Centrifuge experiments conducted in this laboratory allowed the separation of hydrogen isotopes to be thoroughly investigated [51].

It was concluded that for technical reasons centrifuges with partially ionized plasma show little promise. Specifically, it turned out that isotopes of metal elements can be separated only in centrifuges with hot walls, electrodes, and insulators at temperatures sufficient to maintain vapor pressure at the level of $\geqslant 10$ Torr. The number of volatile metals is limited [52], but the novelty of the phenomena being studied was intriguing. Moreover, quite apparent separation effects gave evidence of plasma stability; this unexpected observation also kept the researchers interested and motivated. Most studies were related to model experiments with the use of inert gases and hydrogen–deuterium mixtures.

However, an important disadvantage of centrifuges with *weakly ionized* plasma was documented in the early 1980s [53]. Specifically, some limitations on their separation factor were shown to exist due to a rise in plasma temperature as a result of viscous losses with increasing rotation rate. The maximum value amounts to $\alpha \approx \exp(4\Delta M/\bar{M})$, where ΔM and $\bar{M}$ are the difference between masses of isotopes being separated and their average mass, respectively [54]. At the beginning, the authors of Ref. [54] showed that the main contribution to plasma heating under typical conditions comes from viscous dissipation. Assuming that the plasma cools due to the effect of thermal conductivity of the neutral gas they arrived at the following expression for the separation factor: $\alpha \approx \exp[\Delta M \varkappa/(R\eta)]$, where R is a molar gas constant, $\varkappa$ is the heat conduction coefficient, and η is the viscosity coefficient. Taking into account that $\varkappa/\eta = c_V$ is the gas heat capacity, the authors of Ref. [54] derived the expression for the highest separation factor. The discussion of this issue is to be continued in Section 2.3.

Reference [53] was quickly followed by the first publication on a centrifuge with a *fully ionized* plasma [21]. The expediency of using the fully ionized plasma was substantiated in this study not only by limitations on the separation factor in the case of weak ionization of the gas in the centrifuge but also by another possible problem of bounding from above the ion rotation rate in centrifuge under conditions of partial ionization at the so-called critical level $v_c = (2V_i/M_i)^{1/2}$, where V_i is the ionization potential of neutral atoms.

The existence of critical velocity was postulated by H Alfvén in the 1950s to account for the early stages of the Solar system evolution. It was established in Ref. [55] to be equivalent to limiting the velocity of ions traveling in a neutral gas. On reaching the critical velocity, the energy transferred to ions is spent to ionize the remaining neutral particles. In the English-language literature, the limiting velocity is referred to as the critical ionization velocity (CIV) and is related to developing beam instability in plasma. Theoretically (see review [56]), electrons ionizing neutral particles acquire energy as they interact with waves excited by ions at the lower hybrid frequency $\omega_{LH}^2 = \omega_i^2/(1 + \omega_e^2/\Omega_e^2)^{1/2}$. Here, ω_i, ω_e are the ion and electron plasma frequencies, and Ω_e is the electron cyclotron frequency. The history of investigations into this phenomenon under laboratory and outer space conditions in the period up to the 2000s is traced in Ref. [56].

It has never been observed directly in experimental studies of the separation effect in plasma centrifuges with a partially ionized plasma. The authors of the first study on VACs [21] presented as an experiment with fully ionized plasma reported to have reached the plasma rotation rate in excess of the CIV.

The 2000s witnessed a revival of research interest in centrifugal traps [31] as potential thermonuclear reactors. Experiments with a plasma rotating at a supersonic speed were carried out at the University of Maryland, USA (Maryland Centrifugal Experiment, MCX) (Ellis et al. [57]). The authors recorded, among other things, a limitation on the rotation rate at the CIV level [58].

The Maryland group assumed, starting from Ref. [59], as indisputable the limit for the rotation rate of a fully ionized plasma equal to the Alfvén velocity: $v_\varphi < v_A$ ($v_A = H/(4\pi\rho)^{1/2}$, $\rho \approx n_i M_i$). In the Maryland experiments, this limit was higher than the CIV limit also associated with Alfven's name. In what follows, we leave aside the problem of limiting plasma rotation rate on the grounds that separation of chemical elements with essentially different masses can be addressed within the bounds of attainable rotation rates.

2.2 Experiments with a vacuum-arc centrifuge

2.2.1 Description of experiments. The majority of experiments on the separation of isotopes and mixtures of chemical elements in plasma centrifuges were performed using pulsed centrifuges suitable for the purpose whenever separation can be achieved for a time smaller than the pulse length. A centrifuge operating in the pulse regime does not usually experience a heat impact on its structural elements, which makes possible experimenting at discharge parameters unattainable in the stationary regime under routine laboratory conditions. By way of example, such experiments with a partially ionized plasma were reported in Refs [10, 11]. Certainly, they required a nonstandard approach to pulsed gas sampling from probes for mass spectrometric (MS) analysis [60]. Characteristics of the experimental setup created later proved to be poorer [61–63]. The authors of experiments with a pulsed VAC appear to have been governed by the same considerations. A low-capacity VAC was tested in the stationary regime [64], but the separation effect was not measured.

To begin with, we consider certain methods for excitation of plasma rotation in plasma centrifuges (Fig. 1). One of them is based on transferring the central electrode potential along the external magnetic field and makes use of the strong anisotropic conductivity of the plasma, when a plasma capacitor with the plasma central electrode is formed. In the work mentioned in the present review, such conditions were created in discharges at initial working gas pressures $p_0 < 1$ Torr and longitudinal magnetic fields $H > 1$ kOe. At higher starting gas pressures and lower magnetic fields, the current line distribution becomes similar to that shown in Fig. 1a.

Another method proposed by Lehnert [47] complements the previous one and permits modulating the radial plasma rotation rate profile. It is utilized in the APMF and DIS-1 separator of the Kharkiv Institute of Physics and Technology [17]. It can also be applied to design MCMFs; therefore, we

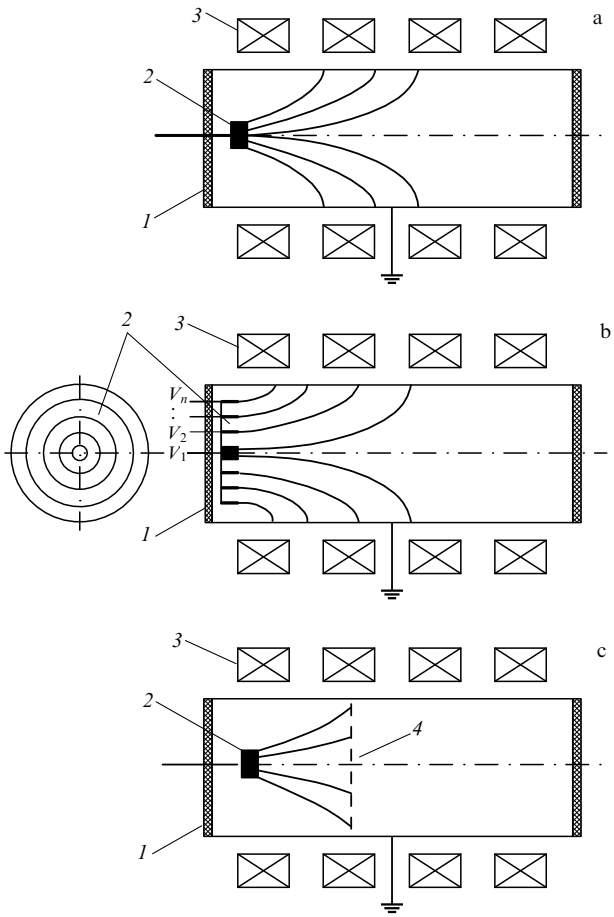

Figure 1. Some modes of plasma rotation driven by direct and pulsed currents: *1* — discharge chamber, *2* — electrode, *3* — solenoid, and *4* — metallic grid; V_1, V_2, ..., V_n — ring electrode potentials. The figure shows putative electric current lines in discharges.

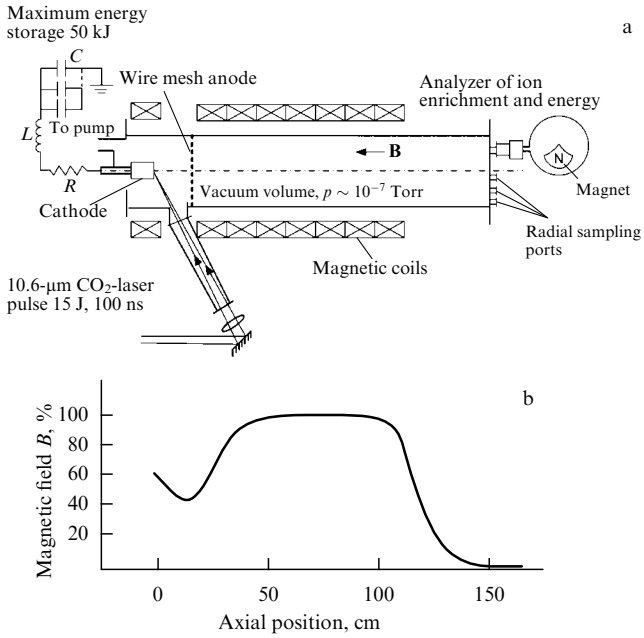

Figure 2. Schematic of a VAC (Yale University, USA) [12].

continue discussing it below though making allowance that in a device operating in the stationary mode it is reasonable to apply this approach with independent ionization of the working substance.

Finally, the nonobvious method illustrated in Fig. 1c was applied in experiments with VACs (except the very first study [21], performed as shown in Fig. 1a). However, taking into account the difference between the areas of the cathode and the corresponding (with regard to magnetic lines) surface of the grid wires provides an explanation for the appearance of the radial component of discharge current triggering plasma rotation upon interaction with the longitudinal magnetic field ($j_r B_z$). The presence of radial current is confirmed by the fact that the diameter of the plasma column behind the grid is larger than cathode diameter [22].

The use of a grid in VACs is mandatory. Unfortunately, none of the publications on VACs refers to this issue. Therefore, it is opportune to remind the reader that in the 1970s Karchevskii and co-workers [65, 66] employed a grid as the anode in high-current discharges and studied the properties of electron beams generated in the discharge gap in the equipotential space behind the grid. We believe that the grid in VACs limits the discharge region as well, and makes possible measurements of parameters of both the plasma and separation effect in the equipotential space. Grids were also used for the same purpose in certain experiments on ICR separation of isotopes (see Section 7). Evidently, the presence of the grid decreases, on the whole, the rotation force $j_r B_z$.

Most experiments carried out to evaluate the VAC separation power were performed with devices based on the design features proposed at Yale University [21]. Neither their parameters nor plasma characteristics were significantly different. We shall describe VAC operations with averaged experimental parameters, disregarding only those characteristic of the more powerful VAC facility at Ibaraki University, Tsukuba (Japan) [67]. Figure 2 gives a typical schematic representation of a VAC [22].

The rotating metal plasma column 4–6 cm in diameter is located in a VAC vacuum chamber up to 2 m long (diameter 15–18 cm) placed inside a solenoid. The length of the section with a uniform magnetic field amounts to 1.2 m. The plasma is generated by ionizing metal vapors produced by cathode erosion in a high-current pulse discharge between the cathode and a wire mesh forming the anode.

The first electric breakdown between the cathode and the grid ($\approx$ 10 cm) occurs upon laser evaporation of the cathode material. The plasma within the discharge gap is driven into rotation, as mentioned in an earlier paragraph (Fig. 1c). The rotating plasma spreads out along the magnetic field into the equipotential space behind the grid where radial separation effect develops at a distance of 60–70 cm away from the grid, as was shown by an analysis of Cu–Ni mixture sediment in different cross sections.

Isotope separation experiments have demonstrated enrichment of the peripheral region of the plasma column with heavy isotope ions, and the paraxial one with ions of light isotopes. With a Gaussian radial distribution of ion density established during plasma propagation in the magnetic field behind the anode grid, enrichment in heavy isotopes at the periphery is much more pronounced than that in light ones in the paraxial region. In terms of the separation process, VACs are described as *concurrent centrifuges* [26, 27].

Initially, the separation effect was estimated from the radial dependence of the ratio between ion isotope concentra-

Table 1. Parameters of a vacuum-arc centrifuge.

Parameter	Value
Longitudinal magnetic field	0.01–0.5 T
Cathode diameter	1.5–2.5 cm
Discharge current	1 – 6 kA
Capacitor bank voltage	$\leqslant$ 5k V
Energy storage of battery	$\sim$ 50 kJ
Discharge time	$\leqslant$ 10 ms
Diameter of plasma column	4 – 6 cm
Ion concentration on column axis	$\leqslant (1-5)\times 10^{13}$ cm $^{-3}$
Ion charge multiplicity Z	2 – 4
Rotation rate of plasma column	20–30 kHz
Longitudinal plasma velocity within column	$\sim 10^6$ cm s $^{-1}$
Amount of substance transferred per pulse	10 – 100 mkg

tions. Ions for MS analysis were extracted through the openings in the end flange (plasma stream receptacle) (see Fig. 2). A sector mass spectrometer for studying pulsed processes was used at Yale University for measuring these dependences [68]. In the other laboratories, quadruple mass spectrometers were employed for the same purpose.

In subsequent experiments, the isotope separation effect was evaluated based on the results of MS analysis of the sediment composition deposited on the plasma receptacle. Secondary-ion mass spectrometry (SIMS) was applied in the analysis. The chemical composition of sediments resulting from alloy separation was determined by electron spectroscopy for chemical analysis (ESCA).

The rotation velocity of the plasma column was usually measured from the phase shift of periodic density fluctuations recorded by electric probes introduced into the plasma with azimuthal displacement. In Ref. [69], the rotation velocity was determined by simultaneously measuring the Doppler shift of spectral lines. It was argued that the angular speed of rotation ω in the plasma column is unrelated to the radius, i.e., the column rotates as a rigid rotor. One of the concluding publications concerning VAC [70] points out that universal drift instability of the plasma is the main cause of density fluctuations. VAC parameters are presented in Table 1.

2.2.2 Results of experiments. In early studies, when the separation power was estimated from relative concentrations of isotope ions, a remarkable result was obtained in zirconium separation experiments. The enrichment evaluated based on a change in the $^{96}Zr^{2+}/^{90}Zr^{2+}$ concentration ratio ($\Delta M = 6$ a.m.u.) from column periphery to its axis amounted to 1700% [71]. Henceforth, this characteristic of the separation effect will not be used, since it contradicts those adopted to describe the separation process. Indeed, the enrichment factor is sometimes expressed in percentage form, as $\varepsilon = \alpha - 1$, but this coefficient is used to characterize the separation process only for $\alpha - 1 < 1$ [72]. In what follows, we shall use for this purpose the separation factor α itself.

Here are the main results of isotope separation experiments performed at Yale University:

— copper isotopes $^{65}Cu/^{63}Cu$, $\alpha \approx 2$ [21];

— zirconium isotopes $^{96}Zr/^{90}Zr$, $\alpha \approx 18$ [71];

— magnesium isotopes $^{24}Mg/^{25}Mg$, $\alpha = 1.2$; $^{24}Mg/^{26}Mg$, $\alpha = 1.3$ [73].

In Ref. [73], the isotope separation effect in magnesium was evaluated based on MS analysis of the samples. Unfortunately, it is unknown whether the strong zirconium separation effect was confirmed by the same method [71].

Table 2. Separation factors α.

Institution	Mixture composition				
	Cu/Ni	Zn/Cu	$^{65}Cu/^{63}Cu$	$^{26}Mg/^{24}Mg$	$^{25}Mg/^{24}Mg$
ANSTO	—	1.4	1.15	—	—
Univ. of Sydney	1.4	—	1.18	—	—
INPE	—	—	—	1.26	1.15
Isomed	—	4	—	—	—
Ibaraki Univ.	—	5	—	—	—

Reference [73] turned out to be the last in the series of Yale researchers' publications about these experiments. Luckily, VAC-based experiments had been initiated by that time at the Institute National de Pesquisas Espatiais (INPE) (Brazil), the University of Sydney, the Australian Nuclear Science and Technology Organisation (ANSTO), the Isomed Co. (Israel), and Ibaraki University, Tsukuba (Japan). Results of experiments performed outside Yale University before 1994 are summarized in review [28]. Table 2, borrowed from Ref. [28], presents separation factors α.

The excellent agreement between the data on Mg isotope separation obtained at INPE and Yale is worthy of special note. However, the high values of copper isotope separation factors ($\alpha \approx 2$) reported from Yale University were not attained in two Australian laboratories.

Directly related to the subject matter of the present review are results of the separation of chemical elements in VACs. Their presentation needs to be preceded by the results of the separation effect calculation [22]. Calculations based on the two-fluid magnetohydrodynamic model of plasma yield the magnitude of the sustained separation effect. As far as the diffusion process leading to the steady-state separation effect is concerned, the authors of Ref. [22] emphasize that it can be estimated in terms of a kinetic theory. Calculations give evidence that the equilibrium radial distribution of ion density corresponds to the Gaussian distribution:

$$n_{\rm i}(r) = n_{\rm i}(0)\,\exp\left(-\beta r^2\right), \tag{1}$$

where

$$\beta = \frac{Z_{\rm i} e}{2k_{\rm B}T}\left[2a - \omega_{\rm i} B_z\left(1 + \frac{\omega_{\rm i}}{\Omega_{\rm i}}\right)\right], \tag{2}$$

$\omega_{\rm i}$ is the rotation rate of the plasma ion component, and $\Omega_{\rm i}$ is the ion cyclotron frequency.

The value of a can be found from the radial dependence of the plasma electric potential:

$$\Phi(r) = \Phi(0) + ar^2. \tag{3}$$

The radial potential distribution in VACs was measured by many authors, including those of Ref. [22].

The formula for the separation factor of a binary mixture of isotopes is identical to that for calculating relevant effects in gas centrifuges:

$$\alpha = \frac{(n_{\rm H}/n_{\rm L})_{r_0}}{(n_{\rm H}/n_{\rm L})_0} = \exp\left(\frac{\Delta M \omega^2 r_0^2}{2k_{\rm B}T}\right). \tag{4}$$

The same formula is applicable to calculating the separation factor of a binary system of chemical elements at $Z_{\rm H} = Z_{\rm L}$. In the case of $Z_{\rm H} \neq Z_{\rm L}$, only the following separation factor is

calculated immediately:

$$q = \frac{(n_{\mathrm{H}}^{1/Z_{\mathrm{H}}}/n_{\mathrm{L}}^{1/Z_{\mathrm{L}}})_{r_0}}{(n_{\mathrm{H}}^{1/Z_{\mathrm{H}}}/n_{\mathrm{L}}^{1/Z_{\mathrm{L}}})_0} = \exp\left[\left(\frac{M_{\mathrm{H}}}{Z_{\mathrm{H}}} - \frac{M_{\mathrm{L}}}{Z_{\mathrm{L}}}\right)\frac{\omega^2 r_0^2}{2k_{\mathrm{B}}T}\right]. \quad (5)$$

These formulas were derived on the assumption that the plasma column rotates about its axis as a rigid rotor: $v_\varphi = \omega r$, and isothermal plasma with pressure $p = nk_{\mathrm{B}}T$ is considered.

Figures 3 and 4 plot radial sediment density distributions on the plasma stream receptacle obtained in Ref. [22] and separation factors of the components of binary Al–Ti and Cu–Ni alloys, which were calculated from sediment composition at different points of the receptacle. It follows from Fig. 3 that separation of the Al–Ti mixture results in the enrichment of the plasma column periphery with light but not heavy components. The Cu–Ni mixture (Fig. 4) is traditionally separated in a VAC, with the heavy component being concentrated at the periphery. The mean charges of the ions (components of the mixtures) were found from the results of MS analysis of the ion stream toward the end wall of the centrifuge (see Fig. 2) to equal 1.97, 4.14, 3.0, and 3.0 for Al, Ti, Cu, and Ni, respectively. Evidently, the concentration of Ti ions on the axis is due to their high charge.

It should be noted that the separation factor $\Delta A \approx 5$ a.m.u. ($\alpha \approx 1.5$) of the Cu–Ni mixture (Fig. 4) obeying centrifugal sedimentation laws is quite different from the separation factor of zirconium isotopes $^{96}\mathrm{Zr}/^{90}\mathrm{Zr}$: $\Delta M = 6$ a.m.u.

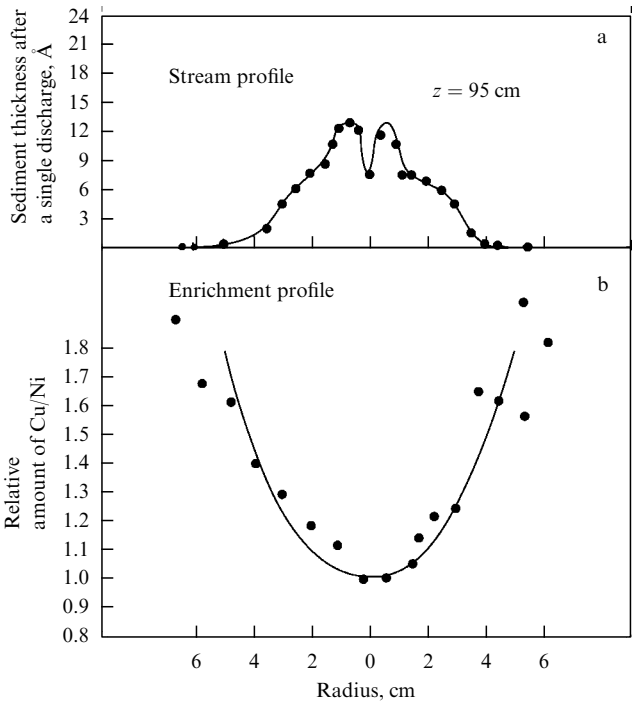

Figure 4. (a) Radial distribution of Cu–Ni sediment thickness. (b) Separation factor [22].

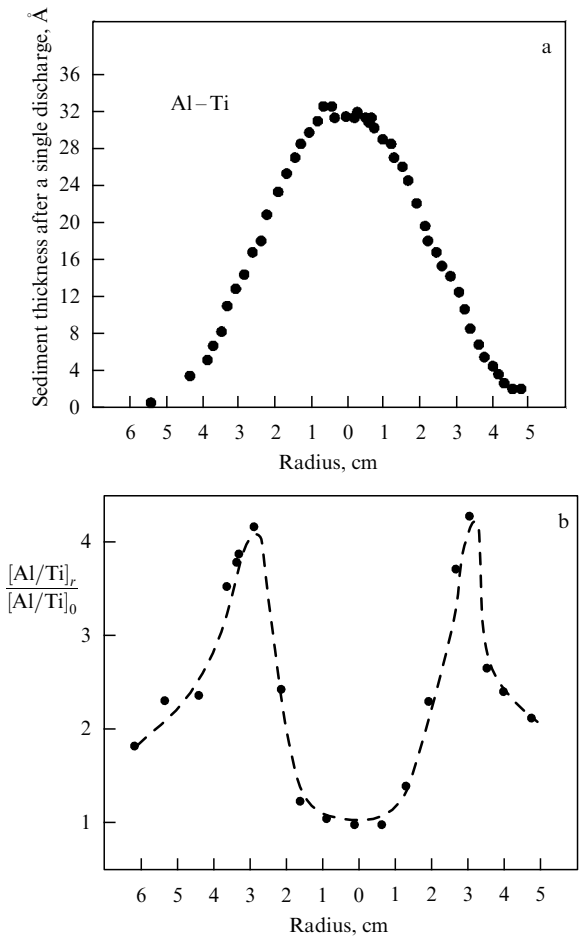

Figure 3. (a) Radial distribution of Al–Ti sediment thickness. (b) Separation factor [22].

($\alpha \approx 18$) [71]. Unfortunately, the latter value (minus unity) was used as a reference for estimating inferred separation factors in a rotating plasma: $\alpha = 10^3$ in the case of separating the ions with masses of 65 and 80 a.m.u. [19].

In our opinion, several circumstances clearly described in Ref. [71] rule out the use of this value as a reference. First, it was deduced from the isotope composition of a Zr^{2+} ion stream accounting for only 25% of the total ion flux (mean zirconium ion charge in the column is $\bar{Z} = 3$). Second, the mass spectrometer was unable to discriminate between signals from different components of the ion isotope mixture. The contribution of each isotope to the recorded integral signal had to be estimated by mathematical analysis. Third, depletion of the paraxial region of the plasma filament in $^{96}\mathrm{Zr}$ and $^{94}\mathrm{Zr}$ isotopes was never equivalent to the enrichment of the peripheral zone with these isotopes. We think that it is more rational to use for predictions the value of $\alpha = 1.3$ ($\Delta M = 2$ a.m.u.) [73] obtained by MS analysis of magnesium samples.

It may be concluded that the separation properties of VACs makes them unsuitable for wide application in isotope technology. A series of experiments were conducted to elucidate factors influencing the plasma rotation rate and temperature [74, 75]. Specifically, the dependence of the rotation rate on geometric and electric characteristics of the wire mesh anode was investigated (Fig. 1c). However, results of these experiments open up no prospects for the further improvement of VAC characteristics.

2.3 Peculiar features of plasma centrifuges

Thus, it turned out that the vacuum-arc plasma centrifuge is far from being as universal a separation device as the gas centrifuge. Paradoxically, light ions are likely to concentrate in the peripheral region of the plasma concurrent centrifuge (see Fig. 3) during separation of some other mixtures of

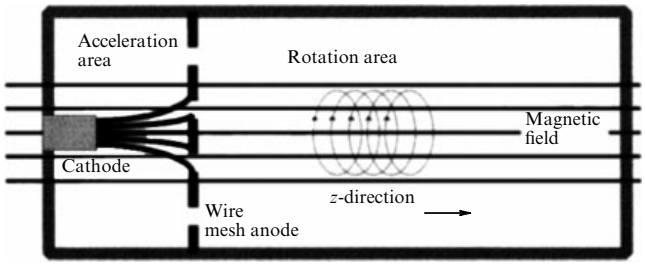

Figure 5. Elementary schematic of a VAC [76].

chemical elements. Moreover, certain mixtures are refractory to separation, e.g., when $Z_H/M_H = Z_L/M_L$ [see formula (5)].

The aforementioned drawbacks of centrifuges should be attributed not only to their design features but also to plasma properties. It is not infrequently maintained that ion separation in electromagnetic fields depends precisely on the Z/M ratio, but this inference is not always taken into account when moving from isotope separation process to separation of chemical elements. The influence of ion charges on the mass separation process will also be discussed in other sections.

Let us consider an elementary schematic of a VAC (Fig. 5) for concluding comments with reference to the steady-state process, starting from the plasma acceleration region. Let an evaporated mixture of RW or SNF components be fed into this zone; also, imagine that all gaseous components (oxygen, nitrogen, etc.) were preliminarily removed from the mixture and it contains only condensable components. Under these conditions, the device operates as a concurrent centrifuge [26, 27]. The mixture is ionized in a DC discharge between the cathode and the wire mesh anode (experiments with lithium vapor ionization in a similar discharge performed in other studies [77, 78] can be regarded as model experiments). The plasma thus formed is accelerated along φ and z coordinates and its rotating stream spreads out to fill the volume behind the mesh.

What knowledge can be deduced from VAC-based experiments? The expansion of the plasma stream in the drift zone is prevented by the external longitudinal magnetic field (Figs 3a, 4a). Additionally, the radial separation effect in the plasma column is apparent behind the mesh over a flight distance of 60–70 cm [22]. The moving plasma volume performs 2–3 revolutions for 100-μs time of flight ($f = 20$–30 kHz, $v_z \sim 10^6$ cm s^{-1}). According to Ref. [22], the frequency of ion-ion collisions is $\nu_{ii} = 10^6 - 10^7$ s^{-1}, which means that the effect of interest shows itself in $10^2 - 10^3$ collisions. Calculations using the formula for ion collision frequency [24]

$$\nu_{ii} \approx 5 \times 10^{-7} \frac{n_i Z^4}{T_i^{3/2} A^{1/2}} ,$$

where n_i is the ion concentration [cm^{-3}], T_i is the ion temperature [eV], and A is the atomic mass [a.m.u.], at $T_i = 1$ eV, $n_i = 10^{13}$ cm^{-3}, $Z = 3$, and $A = 65$ a.m.u., yielded $\nu_{ii} \approx 5 \times 10^7$ s^{-1}.

VAC studies appear to have confirmed the existence of the separation effect in a rotating fully ionized plasma confined by a magnetic field. To recall, the author of Ref. [26] argues that the results of separation in a partially ionized plasma become apparent behind the grid, whereas there are no conditions for the manifestation of the centrifugal separation effect in condensable partially ionized vapor in the acceleration zone before the grid in a cold-wall chamber (see Fig. 5). Notice also that the separation effect is a consequence of collisions between ions with different masses (the aforementioned collision frequencies hold for ions of equal mass).

Turning back to the problem of separation of RW and SNF components in a VAC, it can be expected that these components will be partly separated in the sediment deposited on the cooled receptacle of the plasma stream at the end of the drift zone (see Fig. 5). The magnitude of the separation effect can be predicted based on the separation factor of the Cu–Ni mixture: $\Delta A \approx 5$ a.m.u., $\alpha = 1.5$ (see Fig. 4). Separation patterns can be distorted, because the effect depends on the Z/M ratio [see formula (5)]. An important technical problem covers the service life of the mesh (most probably made from tungsten wire) staying for a long time in contact with uranium plasma.

The paradoxical concentration of the light component at the periphery of centrifuges with a partially ionized plasma has never been recorded. Generally speaking, VACs have an advantage in values of isotope separation factors obtained; however, individual experiments with a partially ionized plasma yielded similarly good results. For example, Ref. [79] reported ^{22}Ne/^{20}Ne separation ($\Delta M = 2$ a.m.u.) of neon in a mixture with hydrogen with the separation factor $\alpha = 1.44$ close to that achieved in ^{26}Mg/^{24}Mg isotope separation (see Table 2). The separation factor in a hydrogen–deuterium mixture was $\alpha = 20 - 25$ [51], and amounted to a few hundred in mixtures of inert gases [10, 11].

A centrifuge with a weakly ionized plasma was found to be hardly suitable for mass separation [53] (see Section 2.1). This fact was specially emphasized by VAC researchers. The authors of Ref. [71] described the article by Wijnakker and Granneman [53] as the 'death knell' for centrifuges with *weakly ionized* plasma. Such a description is incorrect, because it characterizes the mode of centrifuge operation in the low-power regime rather than the device itself. The authors of Ref. [53] showed that plasma heat conductivity and viscosity in the centrifuge are determined by the neutral plasma component and thereby designated the conditions under which their conclusions can be regarded as valid. Clearly, these parameters are increasingly more strongly influenced by both the ion and electron components of the plasma with the growth of discharge power and degree of ionization. Such an influence can be equally well manifested at low degrees of ionization. For example, it was estimated in Ref. [80] that the frequency of ion–ion collisions in inert gases at a temperature of ~ 1 eV and the degree of ionization of only a few percent is already higher than the charge exchange frequency.

In the present review, centrifuges with a potential discharge power in a neutral gas of $\geqslant 50$ kW are referred to as centrifuges with a *partially* ionized plasma (following Ref. [47]). They may fall out of use for technical reasons. It was mentioned above that to work with the vapors of condensable substances, all structures of a centrifuge need to be heated to a temperature at which the saturated vapor pressure of all mixture components is at least 10 Torr. This problem is very difficult to solve for the purpose of RW and SNF processing. Therefore, we address it based on past experience of designing a centrifuge for work with lithium vapors [61–63].

Let us consider creation of the countercurrent flows in the plasma centrifuge. Unlike flows in a gas centrifuge,

countercurrent flows in plasma centrifuges with a partially ionized plasma can develop spontaneously due to the presence of longitudinal temperature gradients and gas deceleration near the ends of the discharge chamber (see Refs [81, 82] for acquaintance with various types of spontaneous circulatory flows). A method for the creation of a controlled counterflow for multiplying the radial separation effect and its conversion into the longitudinal one was described in Bonnevier's article cited above [45]. It is proposed to place a current-carrying conductor on the centrifuge axis to let longitudinal current generate in the plasma an azimuthal magnetic field H_φ decreasing toward the periphery; its interaction with radial current j_r will cause the paraxial plasma to move to the end of the centrifuge and, in as a consequence, in the opposite direction along its wall. This method for inducing circulation was tested in Ref. [83] in a pulsed plasma centrifuge with partially ionized plasma. Turning on the axial current ($\sim$ 10 kA) to separate inert gas mixtures (Ne–Xe and He–Ne) resulted in the desired change to local concentrations of mixture components.

The influence of spontaneous circulation flows was observed in experiments with a stationary plasma centrifuge with partially ionized plasma [61–63]. Longitudinal effects of separation of a gaseous He–Xe mixture and xenon isotopes were documented. The most likely cause of the circulation flow was supposed to be the longitudinal temperature gradient. Separation effects could be diminished by inducing a gas counterflow with the aid of blades attached to the walls of the discharge chamber at an angle of 30° to the cross section plane. Separation effects remained unaltered for reverse plasma rotation (a change in the direction of the external magnetic field), when the plasma streams moved in the same direction. The dynamic pressure of the axial plasma stream originated from the cathode was measured and the velocity of its particles ($\sim 10^5$ cm s^{-1}) estimated in Ref. [63].

This section concludes with the question: "Can plasma centrifuges be used to reprocess RW and SNF?" Technically, one-pass VACs appear to be, in our opinion, the most suitable for further work in this area. Thus far, centrifuges can be utilized to address specific problems, e.g., separation of lanthanide and actinide mixtures. The authors of Ref. [84] propose that this problem be solved with the use of MCMF (see Section 5), although VACs also provide an acceptable alternative.

3. Plasma mass filter

3.1 Physical principles

This section presents a separation device with a rotating plasma (APMF), mentioned in Section 1. It is actually a plasma centrifuge, but the designers considered its centrifugal effect described in Section 2 insufficient for their purposes and planned to reach the desired separation effect predicted for the first time by Okhawa [6] as possible in a plasma centrifuge at a positive electric potential applied to the central electrode or the paraxial plasma region.

The problem of polarity of the voltage inducing the radial current has never been a central one in experiments with plasma centrifuges. It arose, for instance, in the discussion of mechanisms operating in isotope separation, in addition to the centrifugal mechanism [10, 11]. Experiments in the pulse regime carried out at either polarity of the applied voltage yielded essentially similar separation factors. The maximum value of the separation factor ($\alpha > 100$) was measured in a mixture of inert gases at a positive potential on the central electrode (Fig. 1a), when the contribution of cataphoresis was possible. The stationary discharge in a centrifuge with the anode functioning as the central electrode proved unstable [62].

With a positive potential on the central electrode, the centrifugal and electric forces act integrally on an ion in the rotating plasma, making it incapable of confining ions with mass M_i greater than the critical value M_i^c. The latter can be calculated [6] using a one-particle model of rotating plasma.

An ion in the rotating plasma experiences the influence of centrifugal, electric, and Lorentz forces. In equilibrium, the following relation is satisfied:

$$Mr\omega^2 + eEr - er\omega B_z = 0\,. \tag{6}$$

The solution of equation (6) has the form

$$\omega = \frac{\Omega_\mathrm{i}}{2}\left(1 \pm \sqrt{1 - \frac{4E}{rB_z\Omega_\mathrm{i}}}\right). \tag{7}$$

The force balance cannot be established for $4E/(rB_z\Omega_\mathrm{i}) > 1$. For a filter of radius a with a plasma rotating as a rigid rotor and with the potential V_ctr applied to the central region and zero potential on the chamber walls, one obtains

$$M_\mathrm{i}^\mathrm{c} = \frac{ea^2B_z^2}{8V_\mathrm{ctr}}\,. \tag{8}$$

The critical mass of multiply charged ions is the 'equivalent' mass M_i/Z [4]:

$$\frac{M_\mathrm{i}}{Z} = \frac{ea^2B_z}{8V_\mathrm{ctr}}\,. \tag{9}$$

The aforementioned paper [4] describes additional possibilities for separation in APMFs using as V_ctr the sum of constant and alternating potentials: $V_\mathrm{ctr} = V_\mathrm{dc} + V_\mathrm{rf}$. At the same time, it emphasizes putative disadvantages of a 'standard' APMF ($V_\mathrm{ctr} = V_\mathrm{dc}$). One of them, associated with the presence of multiply charged ions, is reflected in formula (9). It is illustrated in Ref. [4] by an example in which $^{90}\mathrm{Sr}^{2+}$ ions could not be removed from ionized RW if the critical mass $M_\mathrm{i}^\mathrm{c} = 75$.

Another disadvantage relates to the low efficiency of the separation device in moderately strong external magnetic fields; it arises from the possibility of the separation effect to manifest itself only at low plasma densities: $\Omega_\mathrm{i}\tau_\mathrm{ii} \gg 1$, i.e., in a small plasma stream experiencing separation. Both drawbacks are eliminable [4]. Calculations in the single-particle approximation showed that application of even infinitesimal additional alternating voltage V_rf at $\omega = \Omega_\mathrm{i}(1 - M_\mathrm{i}/(ZM_\mathrm{i}^\mathrm{c}))^{1/2}$ can destabilize the orbit of an ion and make it depart to the chamber wall. By way of example, alternating voltage with a frequency of $0.63\,\Omega_\mathrm{i}$ will remove $^{90}\mathrm{Sr}^{2+}$ ions from the plasma to the chamber walls. An increase in the external magnetic field B_z and, correspondingly, in the radial electric field E_r will result in enlargement of the plasma stream to be separated. The authors of Ref. [4] noted that there is the opportunity to separate isotopes in an APMF at the ion cyclotron resonance frequency Ω_i ($V_\mathrm{dc} = 0$). Note, however, that a similar method had already been applied by Dawson et al. [85]. Calculations showed that the delivery of resonant ions to the collector in

the alternating field $E_r \propto r$ (such dependence is chosen in the APMF for a constant electric field) required less energy than in a uniform alternating field. Furthermore, it was explained in paper [4] that plasma quasineutrality in APMFs will be maintained by electron current toward the end electrodes, as heavy ions continue to depart to the chamber walls ($M_i > M_i^c$).

In APMFs, plasma is driven into rotation by applying voltage to the end electrodes (Fig. 1b). By the onset of ATG experimental research, the most widely known experiment with the utilization of this plasma rotation method had been that performed at the Institute of Nuclear Physics, Siberian Branch of the Russian Academy of Sciences [86] with the use of a centrifugal trap in the framework of the controlled nuclear fusion (CNF) program. The ion drift velocity $v_\varphi = E_r/B_z$ achieved in this experiment was tens of times more than the Alfven CIV [55].

Ring-shaped electrodes were installed in APMFs to create a radial rotation rate profile in the plasma corresponding to the rate profile in a rigid rotor: $v_\varphi = \omega r$, $\omega = \text{const}$. In the case of such an azimuthal velocity profile, mixture components are separated throughout the entire plasma volume regardless of the location of atomic ionization site [5]. To recall, ring electrodes were offered for the first time for quite a different purpose [47]. Lehnert proposed using this approach to obtain the radial rotation rate profile at which the plasma is not subject to Rayleigh instability (the rotating plasma becomes unstable in the case of the rigid rotor profile).

The mechanism of ring action is rather complicated. An attempt to describe it was undertaken in Ref. [87]. A successful experiment with ring potential transfer into a plugged magnetic trap at a plasma density of $\sim 10^{11}$ cm^{-3} is described in Ref. [88]. The range of the applicability of the law of isorotation [89] and equipotentialization conditions of magnetic lines of force [41, p. 145] are equally important for the elucidation of this mechanism. This issue being beyond the scope of the present review, we shall adhere to the position of the authors of the studies being cited, when it comes to the transfer of electric potential along magnetic lines and to the *isorotation*, considered in Sections 4 and 5.

Another serious challenge concerns plasma stability in separation devices. It was partially resolved by numerous experiments on isotope separation by plasma technologies. Quite apparent separation effects suggest a fairly high stability of the plasma in the currently exploited separation devices.

3.2 Experiments with a demonstration facility

The results of experiments on the separation of mixtures of chemical elements with the Demo test facility have never been published in detail. The onset of experimental studies on inert gas mixture separation and further experiments with admixtures of metal atoms were announced in Ref. [5]. Thereafter, a successful experiment with a mixture of Ag–Au vapors was posted on the ATG website (http://archimedestechnology.com/index.asp). However, this site has been inaccessible since 2006 (see Introduction).It is worth adding that Japanese physicists presented in 2007 indirect evidence confirming the Okhawa effect [90].

The Demo facility was designed to demonstrate physical and engineering solutions behind the APMF using model nonradioactive substances. Figure 6 presents a schematic of Demo discharge device [8] (it does not show the vacuum chamber containing a discharge device). The total volume of

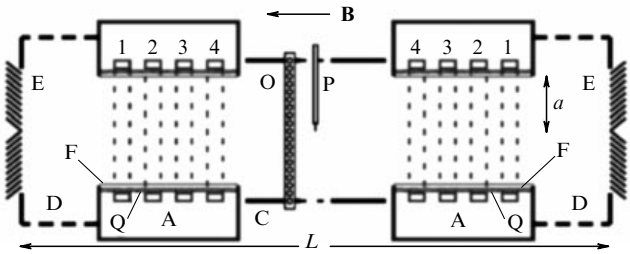

Figure 6. Schematic of the Demo facility [8]: 1–4 — antenna coils, A — cavity for antenna coils with differential pumping, **B** — external magnetic field, C — collector of heavy particles, D — diaphragm, E — electrodes, F — Faraday shield, O — optical windows, P — probe, and Q — quartz tube; L — length of the plasma column, and a — its radius,

the evacuated system was 16 m^3. The vacuum chamber was placed in a longitudinal magnetic field with induction $B \leqslant 1600$ Gs, which was uniform within 2% of the volume occupied by the plasma.

An important breakthrough was the creation of a large-diameter plasma column (≈ 80 cm) by helicon-induced ionization (helicons are circularly polarized waves propagating in a plasma in the frequency range from ω_{ci} to ω_{ce}). This ionization modality proposed by Boswell [91] was formerly applied only in small laboratory setups [92, 93] with the use of a dielectric shell (boron-silicate or quartz tube insulating the plasma from high-frequency (HF) induction antennas. This quartz shell (Q in Fig. 6) was also used at Demo. The power of the HF generator feeding the antennas amounted to 4 MW. The HF oscillation frequency in Demo experiments was as high as 6 MHz. The authors of Ref. [8] consistently emphasize that Demo is the world's biggest facility with a helicon discharge according to the initial scheme [91]. Argon plasma density at a starting argon pressure of 16 mTorr and HF discharge power of 628 kW reached 1.5×10^{13} cm^{-3}. The electron temperature ranged 2–4 eV (the argon ion temperature being unknown).

Assemblies of 10 concentric rings E each (Fig. 6) were arranged at the ends of the vacuum chamber to drive the plasma into rotation (Fig. 1b). Power supply sources maintained potentials up to 700 V at the rings. Probing showed that up to 80% of the ring potential was transmitted to the plasma [5]. The observed rotation rate proved lower than expected, but its radial profile matched that of a rigid rotor. Parabolic potential distribution was maintained at the rings to create such a profile.

The RW separation process designed to be put into effect based at an industrial-scale plant was posted on the ATG website. Waste in the form of melt microdroplets is injected into the plasma preliminarily formed in the mid-plane of the installation. Then, the substance of interest evaporates, its atoms are ionized and involved in rotational motion, while the plasma can no longer confine radioactive ions with mass $M_i > M_i^c$ (see formulas (8) and (9)), which go to the walls of the chamber and concentrate in the collector of heavy particles. Light ions with mass $M_i < M_i^c$ remain confined till they deposit on the end electrodes that also serve as their collectors. What component of this mechanism proves defective is unknown. It can be speculated that separation occurs only at low plasma densities, which makes unpromising prospects for the practical application of this separation technique. The inventors of the MCMF consider low efficiency to be the chief shortcoming of the APMF [20].

A rough estimate of the possible mass flow in a Demo type unit with the plasma column cross section $S \approx 4 \times 10^3$ cm^2 [8] can be obtained using plasma density and electron temperature measured in experiments with argon, $n \sim 10^{13}$ cm^{-3}, $T_e = 4$ eV, and assuming the speed of ion propagation toward the unit's ends to be $v_z = (T_e/M_i)^{1/2} \approx 2.5 \times 10^5$ cm s^{-1} ($M_i = 65$ a.m.u.). Under these conditions, as much as ~ 100 kg of light RW can be transferred in the plasma column on a daily basis. A commercial grade unit with a waste processing capacity of roughly 700 kg/day was being designed [5] in parallel with Demo experiments, probably because such an approach was once deemed infeasible and impracticable for the treatment of such large amounts of RW. This may have been the main reason for ATG to suspend its activities related to RW processing. It should be borne in mind that at $T_i \sim 1$ eV and the aforementioned plasma densities ($\sim 10^{13}$ cm^{-3}) and magnetic field ($B \approx 0.2$ T) even singly-charged ions escape magnetization ($\omega_{ci}\,\tau_{ii} \sim 1$), which means that the magnetized plasma density must be lower than that in accomplishing the separation process.

4. Magnetoplasma separation techniques

4.1 Experiments with mass filters

Reprocessing of RW and SNF is an especially challenging task for Ukraine, where almost 50% of the electric power comes from nuclear power plants [16]. Experiments on magnetoplasma separation simulating RW and SNF treatment were carried out at the Kharkiv Institute of Physics and Technology [17, 18]. In the 1970s, they resulted in the discovery of selective ion heating at $\omega_E = \omega_{ci}/2$ [12]. The authors attributed this phenomenon to the development of ion cyclotron instability, discussed in greater detail in Section 4.2.

Ongoing experiments have the objective to more thoroughly study the plasma mass filter in which the ion critical mass M_i^c is defined by the same relation $\omega_E = \omega_{ci}/2$ (Section 3.1). A positive electric potential needs to be maintained on the axis of the rotating plasma column, whereas the authors of Ref. [12] applied a negative potential to the paraxial plasma volume to induce rotation. A schematic of their DIS-1 separator is presented in Fig. 7 [94].

An assembly of nine concentric ring electrodes (*4*) is deployed to ensure the plasma rotation (Fig. 7). The total voltage across the rings is $U = 0-240$ V ($E_r = 0-12$ V cm^{-1}). A positive electric potential maintained on the axis enables the unit to operate as a mass filter (see Section 3), but mixture ionization and separation zones are spaced apart, unlike those in APMFs. It was expected that ions with mass $M_i > M_i^c$ will escape from the rotating plasma stream as it spreads out within a certain cross section of the decreasing magnetic field, when $\omega_E = \omega_{ci}/2$. The end (*5*) and longitudinal (*6*) ion collectors of DIS-1 (Fig. 7) are designed to record ion fluxes longitudinal and transverse with respect to the magnetic field, respectively. Sector (lamellar) collectors trace flow intensity distribution along the setup radius and length. The magnetic field of the source (*2*) is directed oppositely to the main field for eliminating the mutual transfer of electric potentials between electrodes of the source and the system of ring electrodes (*4*). According to Ref. [95] DIS-1 can be converted into an ICR separator (see Section 7).

Experiments with inert gas (Xe, Kr, Ar) [17, 18] and nitrogen [94, 96) plasmas in electric and magnetic fields

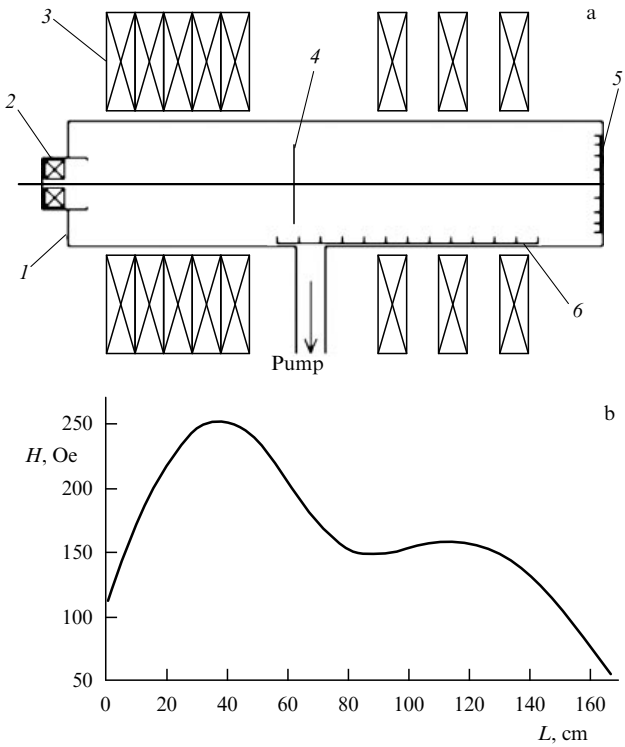

Figure 7. (a) Schematic of the DIS-1 separator [94]: *1* — vacuum chamber, *2* — plasma source, *3* — solenoid, *4* — ring electrodes, *5* — end ion collector, and *6* — longitudinal ion collector. (b) Distribution of the magnetic field strength along the axis.

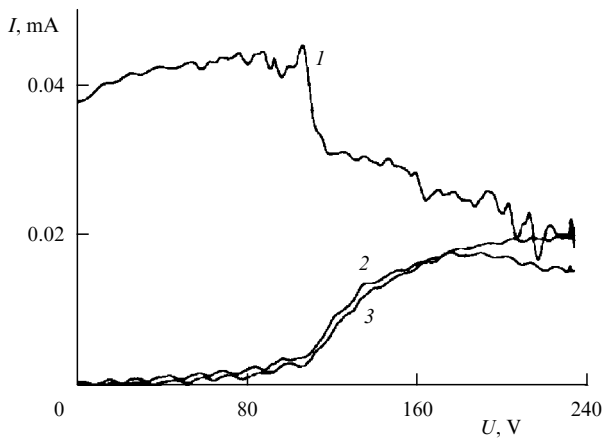

Figure 8. Currents onto the end and longitudinal collectors versus voltage applied to the coaxial electrode system [96]: *1* — current onto the first lamellar section of end collector, *2* — current onto the first lamellar section of longitudinal collector, and *3* — current onto the second bar (lamel) of longitudinal collector.

satisfying the relation $\omega_E = \omega_{ci}/2$ demonstrated the plasma escape to the chamber walls. Figure 8 shows signals coming to the end and longitudinal collectors in the nitrogen plasma where molecular N_2^+ ions were registered.

Experiments with gases fail to comprehensively demonstrate the work of the unit as a mass filter; hence, the necessity of experiments with ionized vapor plasma [18], e.g., alkali metal and calcium vapors, in which particles escaping from the plasma are deposited onto and concentrated in collectors. Evaluation of threshold concentrations of impurities below

which the device remains efficient is as important as the standard problem of its working capacity.

4.2 Experiments in the presence of resonant ion cyclotron instability

In the late 1960s, researchers at the Kharkiv Institute of Physics and Technology discovered instability in a rarefied plasma rotating in crossed electric and magnetic fields, which they called resonant ion cyclotron instability (ICI) (Rozhkov et al. [97, 98]). The phenomenon was apparent at the plasma rotation rate $\omega_E \approx \omega_{ci}/2$ (here is a formula [99] convenient for making 'practical' estimates: $\omega_{ci} \approx 10^4\, ZH/A$ [Oe (a.m.u.)$^{-1}$]). Instability manifested itself as intense plasma oscillations at the ion cyclotron frequency and its harmonics and as the removal of accelerated ions from the discharge along the magnetic field direction. The energy of such ions ranged 100–200 eV.

In Section 3.1, we emphasized the hydromagnetic stability of the plasma in experiments on isotope separation in plasma centrifuges. The present section deals with current and kinetic instabilities that may have positive consequences, such as collisionless turbulent plasma heating [100].

The experimental setup for the study of ion heating associated with the development of resonant ion cyclotron instability is schematically depicted in Fig. 9 [101]. The excitable discharge was a variant of reflective (Penning) discharge, in which cylindrical cathodes are used (shown conventionally in the figure). With this electrode configuration (cylindrical cathodes and anode of identical diameter), the reflective discharge occurs upon a sharp decay of the magnetic field at the edge of the solenoid. This was achieved by applying the ferromagnetic shield. Although the authors of Refs [97, 98] did not disclose details of the shield configuration, it may be conjectured that the latter was similar to that described in Ref. [102].

The cylindrical electrodes were 80 mm in diameter, the gap between the cathodes and the anode $\delta = 40$ mm, and anode voltage $V_A \leqslant 2$ kV (the strength of the radial electric field was calculated using formula $E_r = 0.3\, V_A/\delta$ derived from the estimated electric field distribution between the cathodes and anode in a vacuum). The magnetic field induction was $\leqslant 0.3$ T, starting working gas pressure $3\times10^{-6}-7\times10^{-4}$ Torr, and plasma density $4\times10^9-5\times10^{10}$ cm^{-3}. The working gases comprised nitrogen, oxygen, argon, helium, and their mixtures.

The authors of Ref. [97] called 'critical' the values of the electric and magnetic fields at which ICI developed

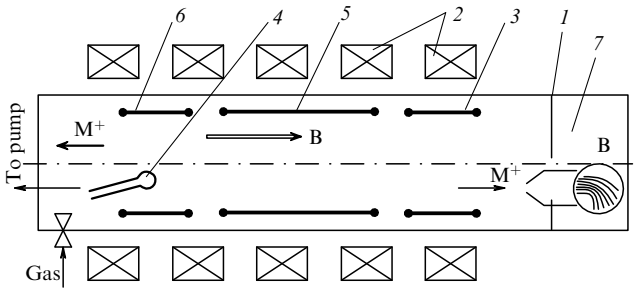

Figure 9. Schematic of the setup in which resonant ion cyclotron instability was observed [101]: *1* — vacuum chamber, *2* — coils generating external magnetic field, *3*, *6* — cathodes, *4* — incandescent cathode, *5* — anode, *7* — enclosure for probes and mass-spectrometer.

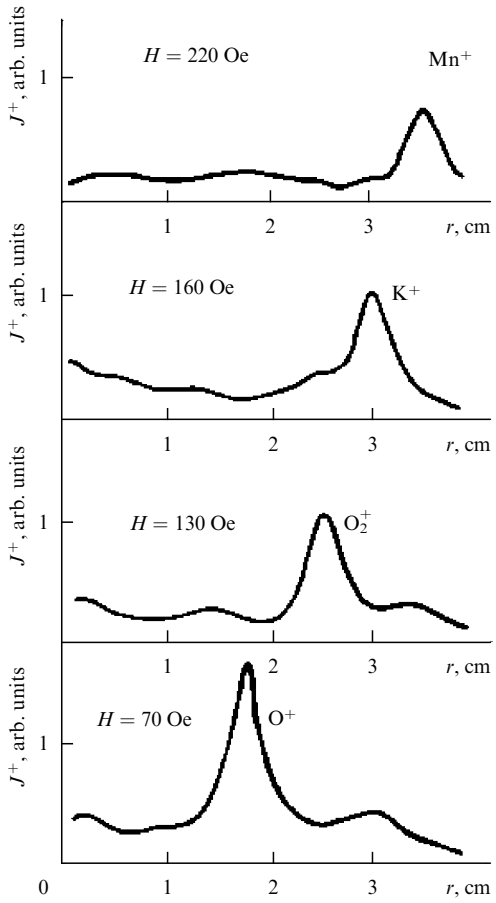

Figure 10. Radial dependences of the yield (J^+) of ions having different masses along the magnetic field in the course of development of resonant ICI [101].

($\omega_E = \omega_{ci}/2$), e.g. $H_c = [2M_i c^2 E_c/(er)]^{1/2}$. The plasma oscillation amplitude at the ion cyclotron frequency and its harmonics sharply increased for $H \geqslant H_c$, while the oscillation frequency for $H \leqslant H_c$.

The selectivity of ion heating in the course of ICI development was studied in Ref. [12], but the data obtained in a later paper [101] appear to be even more illustrative. Figure 10 shows radial dependences of the signals from the receiver of the mass spectrometer (*7* in Fig. 9) at different external magnetic fields (potassium and manganese ions were recorded after adding K_2MnO_4 vapors into the gas discharge). Evidently, favorable conditions for selective heating develop for ions having different masses in cylindrical layers of various radii. ^{7}Li- and ^{6}Li-enriched sediments were obtained on the cooled collector. In these experiments, LiF vapors were added to the gas discharge.

The authors of Ref. [103] tend to believe that instability in a rotating plasma is a result of electron and ion motion relative to each other: they move in rotating plasma with different speeds in crossed electric and magnetic fields due to the difference between centrifugal forces. After this transverse ('diamagnetic') current reaches a threshold value, it can excite plasma oscillations. However, in a high electric field, $E_r \gg E_c$, where resonant ICI is still observable, only oscillations with frequency $\omega > \omega_{ci}$ could be induced, in accordance with the theory. It was shown later in Ref. [104] that under these conditions not only high-frequency oscillations but also long-wavelength oscillations

can develop at the ion cyclotron frequency and its harmonics.

Have other groups observed analogous phenomena? No, at least not in a rotating gas-discharge plasma, though a similar effect was noticeable in a Q-machine (a device for producing a quiescent plasma by surface ionization of atoms on a hot tungsten or rhenium plate) [105] (University of California, Irvine, USA). The excitation of electrostatic ICI [106] and heating of barium ions were reported in Ref. [105], where instability induced by a longitudinal current was reported as a threshold phenomenon. Also, electrostatic oscillations excited by an external antenna were shown to cause ion heating. The heating of K^+ ions in a Q-machine at frequencies $\omega = n\omega_{ci}$ $(n = 1-13)$ was documented in Ref. [107]. With stronger excitation, the heating occurred even at half-integer cyclotron harmonics ω_{ci}, $n = 3/2$, $5/2$, $7/2$, although the harmonic with $n = 1/2$ was disregarded in these experiments. Ion heating at a frequency of $\omega_{ci}/2$ was observed later in Ref. [108], where helium ion isotopes $^3He^+$ and $^4He^+$ were heated in a krypton plasma using an external antenna (helium of an artificial isotope composition was added to krypton).

A concluding remark reduces to the following: experiments with resonant ion cyclotron instability and the excitation of electrostatic ion cyclotron waves were carried out at a low density of resonant particles ($\leqslant 10^{10}$ cm^{-3}).

4.3 Experiments with dense rotating plasma

Experiments at the Kharkiv Institute of Physics and Technology with a reflective discharge in a conventional geometry characteristic of Penning's discharge are conducted based on the 'Maket' facility [109–111]. Such an electrode geometry combines these experiments with those performed in the 1970s, when a plasma centrifuge with two opposite cathodes was proposed as a device with weakened internal secondary flows [112]. The pulsed discharge was roughly 1 ms in duration. The cathodes 10 cm in diameter were either made from or coated with titanium. The discharge was induced in hydrogen and argon at a gas pressure of 0.1–5 Pa and discharge current up to 2 kA. The breakdown was followed by dispersal of the cathode material in the auxiliary gas, after which the plasma titanium concentration amounted to almost 50%.

Major experimental data were obtained by dual-frequency microwave reflectometry: microwave radiation completely reflected from the plasma layer at frequencies lower than the electron plasma frequency $\omega_{pe} = (4\pi n_e^2/m)^{1/2}$. Reflective layers had electron density $n_{e1} \geqslant 1.7 \times 10^{13}$ cm^{-3} and $n_{e2} \geqslant 6.5 \times 10^{13}$ cm^{-3} (the wavelengths of the reflected radiation were $\lambda_1 = 8$ mm and $\lambda_2 \approx 4$ mm, respectively). Regular fluctuations of plasma-reflected signals were observed. Reflectometers placed in the same cross section plane but displaced azimuthally measured oscillation phase shifts that were utilized to calculate the rotation velocity of the plasma electron component ($v_1 \approx 3 \times 10^6$ cm s^{-1} and $v_2 \approx 10^6$ cm s^{-1}) in layers with densities of n_{e1} and n_{e2}, respectively. The reflectometers were also used as locators to measure the radii of cylindrical layers ($r_1 = 5$ cm and $r_2 \approx 4$ cm). It was concluded based on these data that $\omega_1 > \omega_2$; in other words, the plasma electron component rotates in a manner different from that of a rigid rotor.

The analysis of oscillation spectra of microwave radiation signals reflected from the plasma revealed lines corresponding to ion cyclotron frequencies (the ion composition was retrieved from optical spectra). The authors of the experiments attributed these oscillations to the development of electrostatic ICI (therefore, to the excitation of electrostatic ion cyclotron waves (see monograph [106])). It should be noted in connection with the discussion in Section 4.2 that this instability in the above experiments was merely an accompanying phenomenon that is unlikely to produce separation effects additional to the centrifugal one.

Unfortunately, this construction can hardly be regarded as a separation cell for metal chemical elements (instead of gases). Even if the materials of two cathode are dispersed in the cell, there is no case for condensation of either the heavy or light fraction of the separated mixture.

5. Asymmetric centrifugal trap

5.1. Centrifugal traps

As was mentioned in Section 2.1, the 2000s witnessed a revival of interest in the application of magnetic centrifugal traps for confining thermonuclear plasma. Although Ref. [86] was cited as the final publication reporting experiments in the CT-specific geometry of the magnetic field and summarizing results of previous studies, it was followed by new research based on conventional magnetic mirror machines. The system of ring electrodes (Fig. 1b) was no longer used to rotate the plasma; it was substituted by an extended axial electrode. Nevertheless, no signs of developing hydromagnetic instability were observed, even for an uncontrolled azimuthal velocity profile. Measurements of radial rotation rate distribution revealed a stabilizing shear (dv_φ/dr) [113]. Plasma density in the trap was by an order of magnitude greater than that behind the magnetic and centrifugal mirror [114]. In the successful period of these studies, a magnetic centrifugal mass filter (MCMF) was proposed [19, 20] and *asymmetric* centrifugal trap (ACT) was proposed to serve as the filter [32]. Experiments with the exploitation of an ACT have not yet been reported, and the aforementioned CT studies remain the sole source of empirical data for further research.

5.2 Magnetic centrifugal mass filter

The developers of the new mass filter (MCMF) (Fig. 11a) emphasized its two advantages over the APMF: one being the higher efficiency ensuing from the use of denser plasma, the other the independence of the separation process of ion charge Z_i. The potential of the filter was clarified in further studies [115], which showed that the working plasma density in the MCMF is bounded from both above and below (see Section 7.3) and that the calculations hold only for plasma containing no multiply charged ions. The height of the centrifugal barrier for an ion is unrelated to its charge, but charge multiplicity is by no means unimportant for the processes running in MCMFs. It was expected that the plasma in ACTs would be driven into rotation by applying a potential to the concentric rings or by radio-frequency fields [116]. For comparison, Fig. 11b presents a schematic diagram of the CT [117].

Plasma rotation in the magnetic field having configuration shown in Fig. 11a prevents ion departure along magnetic lines of force in the direction of decreasing radius of the hollow plasma structure, because the particles experience the influence of the growing centrifugal force. By choosing a proper plasma rotation rate ω_E, it is possible to determine the boundary mass whose exceeding will not allow such ions to

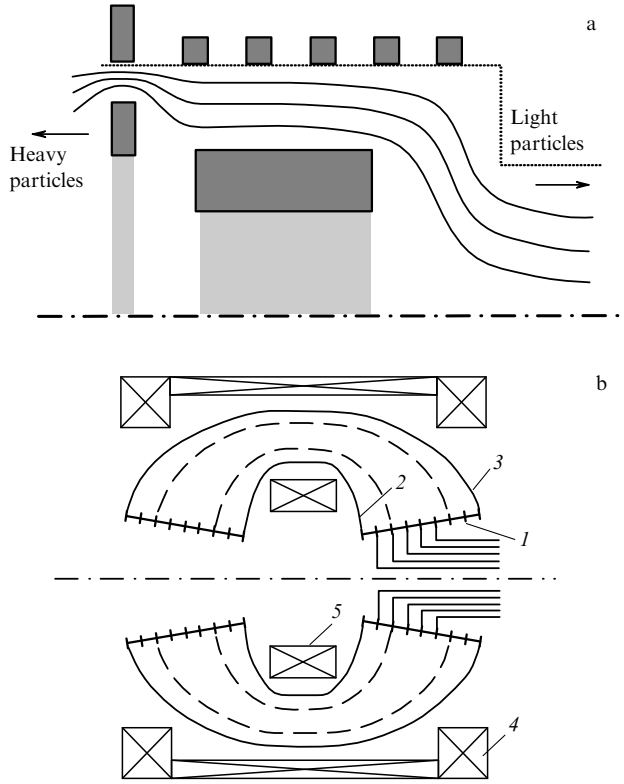

Figure 11. (a) Schematic of MCMF [20]: shaded rectangles show position of magnetic field coils, solid curves — magnetic lines, dotted lines — vacuum volume boundary, and dashed-dotted line — axis of symmetry. (b) Schematic of centrifugal trap [117]: *1* — ring electrodes, *2* — inner chamber wall, *3* — outer chamber wall, *4* — external magnet, and *5* — internal magnet. Dashed curves fit magnetic lines of force.

overcome the centrifugal barrier. Heavier particles are reflected back from the barrier and escape from the opposite side of the trap either directly through the magnetic mirror or through the exit cone after a series of collisions. On the other hand, ions with mass less than the boundary one will be able to penetrate through the centrifugal barrier. Thus, light particles move to the right and heavy ones to the left, as they leave the MCMF (Fig. 11a).

The condition for particle reflection from the centrifugal barrier takes the form [115]

$$\frac{M_{\mathrm{L}}}{2}\,(1 - R_{r_{\mathrm{L}}}^{-1})\,\omega_E^2 r_0^2 \geqslant T_{\mathrm{i}}\,. \tag{10}$$

Here, ω_E is the rate of rotation driven by the electric drift, r_0 is the initial radial position of the ion, $R_{r_{\mathrm{L}}} = (r_0/r_{M_{\mathrm{L}}})^2 \geqslant 1$, and $r_{M_{\mathrm{L}}}$ is the radius of the respective line of force in the light particle exit cross section. At temperature $T_{\mathrm{i}} \sim 10$ eV, the boundary mass at the level of the strontium mass may be set at the rotation rate $\omega_E r_0$ of several kilometers per second [115].

On the opposite (left) side, the light particles are kept confined by the magnetic mirror. The condition of reflection from the mirror for an ion born at point (r_0, z_0) is given by the expression

$$\mu B_0 (R_{B_{\mathrm{H}}}^{-1} - 1) \geqslant \frac{M_{\mathrm{L}}}{2}\,(R_{r_{\mathrm{H}}}^{-1} - 1)\,\omega_E^2 r_0^2\,. \tag{11}$$

Here, $R_{B_{\mathrm{H}}}^{-1} = B_0/B_{M_{\mathrm{H}}} \leqslant 1$ is the ratio of magnetic field B_0 at point (r_0, z_0) to the maximum magnetic field $B_{M_{\mathrm{H}}}$, $\mu = W_\perp/B$, $R_{r_{\mathrm{H}}} = (r_0/r_{M_{\mathrm{H}}})^2 \leqslant 1$, and $W_\perp$ is the energy of ion movement across the magnetic field. The conditions for particle confinement in CTs were formulated for the first time by Boyer and co-workers [118].

Clearly, the direction of movement of the light and heavy fractions of the separated mixture leaving the trap (Fig. 11a) implies that the power supply source must be located inside the filter. References [19, 20] presenting an MCMF separator (Fig. 11a) contain no information on the mode of mixture ionization. It is impossible to use the ring system (Fig. 1b) simultaneously for ionization of the working substance and for driving plasma rotation, because the filter functions as a plasma trap. A later study [84] demonstrated the possibility of ionization in MCMFs by helicons, as well [91].

It is conceivable that ionization in MCMFs (as in APMFs) can be induced by helicons, or a widespread method for vapor ionization by electron cyclotron resonance discharge (ECR-discharge) [119]) is used. But the trap must not contain a cloud of vapors of the mixture to be separated, since it becomes the target of ion charge exchange that impedes the separation process in the MCMF. This suggests the necessity to ionize the mixture of interest in a separate chamber, from which it must be injected into the MCMF. Reference [20] mentions plasma injection along magnetic lines of force, but both this and subsequent studies discuss only the injection into the MCMF of the mixture being separated in the form of ions. Reference [115] indicates a specific point (r_0, z_0) into the vicinity of which the ions should be injected. The point is located close to the exit site of light particles.

The PPPL group initiated experimental studies of the processes forming the basis of the proposed mass filters [120]. Hopefully, they will contribute to the choice of the final design of the MCMF.

In conclusion, Ref. [115] reports the separation factor $\alpha \approx 2$ for an ionized Al–Sr mixture passing through an MCMF, which was calculated on the assumption that $\omega_E \ll \omega_{\mathrm{ci}}$ and that the mixture contains only singly-charged ions. Plasma density was $\sim 10^{12}$ cm^{-3}, and $\approx 15\%$ of the ions were lost in the filter. The separation factor for the passage of an ionized mixture of lanthanides (average mass in uranium fission products $\bar{A} = 144$ a.m.u.) and actinide ^{241}Am through the MCMF was calculated in Ref. [84] (the burning of americium and neptunium as the most dangerous components of the SNF was discussed in Ref. [121]). The result is $\alpha \approx 3$ (particle losses $< 15\%$). Plasma transfer in a magnetic field is considered in Section 7.3.

6. Plasma-optical separation techniques

6.1 Plasma-optical mass separation method with electrostatic focusing

The application of POMS for SNF processing was first proposed in Ref. [13], with reference to so-called panoramic separation, i.e., the removal of individual chemical elements from the mixture (possibly with an EM separator, despite its low efficiency). The author of Ref. [13] intended to use a stationary plasma engine (SPE), creating a plasma stream with the equivalent ion current density of ~ 1 A cm^{-2} [13, 41]. The plasma left the SPE as an axisymmetric hollow flux, exactly such that is needed for the work of a plasma-optical mass spectrometer. Figure 12 presents a diagrammatic layout of a mass separator with electrostatic focusing (POMS-E) [36].

The key element of a POMS is an azimuthator, i.e., a magnet with a radial magnetic field in the gap installed at the

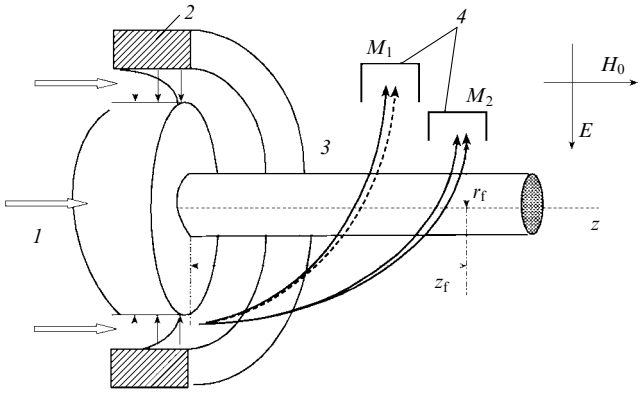

Figure 12. Schematic of POMS-E [36]: *1* — ion source, *2* — azimuthator, *3* — separation region, and *4* — ion collector.

entrance (*2* in Fig. 12). It was calculated that ions in the plasma stream passing through the azimuthator slit convert part of the kinetic energy of directed motion into rotational energy ($v_{z0}^2 = v_\varphi^2 + v_z^2$) and acquire the next azimuthal velocity $v_\varphi = Ze/(cM_\mathrm{i}R)\,\psi$, where ψ is the magnetic flux in the azimuthator, and R is the mean radius of the annular slit. Ions after passing the azimuthator enter the separation region (*3* in Fig. 12), where a radial electric field E_r is created in a cylindrical capacitor (the outer cylinder is not shown). Transitivity, i.e., the maintenance of vacuum distribution of the electric field in the plasma, as well, was planned to be ensured by generating a weak magnetic field in the focusing area that would have no effect on ion movements. Field E_r in plane (r, φ) can focus the ion flux when displaced through angle $\pi/\sqrt{2}$ (a Hughes–Rozhansky energy analyzer [48, p. 35]). Radii r_f of the focusing rings (for an axisymmetric ion source) are determined by equilibrium conditions $M_\mathrm{i}v_\varphi^2/r = ZeE_\mathrm{r}$.

On the strength of relation $v_\varphi \propto 1/M_\mathrm{i}$, the focusing rings for ions of various masses will have different radii. The authors of Ref. [122] were the first to point out this fact, i.e., the dependence of the focusing properties of such a system on ion mass. References [13, 36] report the results of calculations of the trajectories of monoenergetic ions with masses 80, 120, and 160 a.m.u. in the POMS-E. It was found that focusing rings for the beams of these ions having radial deflection $\pm 2.5°$ are spaced z_f apart in one plane (not shown in Fig. 12).

The problem of SNF processing with the aid of a POMS-E was addressed in the research conducted at Irkutsk State Technical University [37, 123–125]. The authors of these publications proposed a modified device (POMS-E-3) compatible with the source of nonmonoenergetic ion flux for separation of three-component mixtures [123]. The end receptacle and the cylindrical capacitor surfaces served as fraction collectors. This device was recommended for the processing of SNFs containing three groups of elements with mass numbers 85–106, 134–155, and 235–244 [37]. The first two groups included fission products, and the third one comprised the residual fuel and actinides formed.

In model experiments [124], a mixture of three gases (nitrogen, argon, and krypton) was ionized in a plasma source. Probing failed to reveal the distribution of ion current in the separating space, indicative of separation into components. It was established in Ref. [125] that the plasma acquires a positive space charge as it passes through the azimuthator, which means that some of the electrons are cut off (external fields E_r and H_z in the separation zone were not generated in these experiments). It proved possible to compensate for the space charge by thermoelectron emission from an additional tungsten cathode, suggesting the possibility of a more successful experiment on separation of the mixture of interest. To recall, the experiments were carried out with a low-density plasma ($\sim 10^9$ cm^{-3}).

The interaction of plasma bunches with the transverse magnetic field was studied in earlier CNF research, e.g., in Ref. [126]. Those were hydrogen plasma bunches with admixtures of carbon, aluminum, and iron ions. Such a magnetic barrier was shown to have a separation potential of its own: the passage of bunch ions depended on their charge and mass.

6.2 Plasma separator with a potential well

The plasma separator with a potential well [38] was proposed collectively by researchers from the Joint Institute for High Temperatures, Russian Academy of Sciences, and the Moscow Institute of Physics and Technology. To illustrate the practicability of this device for SNF processing, the authors of Ref. [38] calculated separation factor of a binary system of singly-charged ions with masses of 240 and 150 a.m.u. as a model of separation of actinides and fission products in a separator. They proposed separators with azimuthal and axial magnetic fields. We shall consider the separator with azimuthal magnetic field

Figure 13a plots ion paths in the azimuthal magnetic field produced by axial current $I(r = 0)$ flowing in the direction of negative $z(H < 0)$ values. Figure 13b presents the distribution of the electric field potential (potential well) exemplified by dimensionless potential $\Pi = U/U_\mathrm{D}$, where $U_\mathrm{D} = W_\mathrm{D}/e$ (index D marks characteristic values of the potential and ion energy). The ion energy $\varepsilon = W/W_\mathrm{D}$, the initial energy $\varepsilon = 10^{-4} - 10^{-3}$, and the extreme trajectories in Fig. 13a correspond to the maximum initial energy of ions $\varepsilon_0 = 10^{-3}$ at angles of $\pm\pi/4$.

The separation process is illustrated for the initial ion energies of 0.1–1.0 eV: in this case, $|U|_\mathrm{max} = 415$ V, and $I = 245$ kA. In the $\sim 0.15a$ section of z (a is the characteristic length), ions are accelerated to an energy of ~ 40 eV; accordingly, the angle and energy spread of data decrease. Thereafter, light ions return to the end wall ($z = 0$), while heavy ones find themselves in the potential well, the depth and position of which were specially chosen to obtain this effect. The heavy ions continue to move toward the z-axis. In the beam cross section shown by the loop (Fig. 13a), the ion energy is 110 eV. The magnetic field strength (H_φ) must be strong enough to enable ions with an energy of several dozen electron-volts to return onto the starting plane with $z = 0$.

Potential well formation is shown in Fig. 14 presenting a sketch of a separator with an azimuthal magnetic field. Electrodes (*3*) generating an electric potential along magnetic lines of force must be in contact with the plasma. The creation of such 'auxiliary' plasma is not discussed in Ref. [38]. It may be suggested that it will be formed simultaneously with the ion flux to be separated. Plasma sources are shown in Fig. 14 (*6*).

The authors demonstrated in a later study [127] that injection of an ion beam along the radius allows separating the same ion mixture in the separator with an azimuthal magnetic field and a radial electric field using no potential well, merely by the choice of a proper radial electric potential distribution.

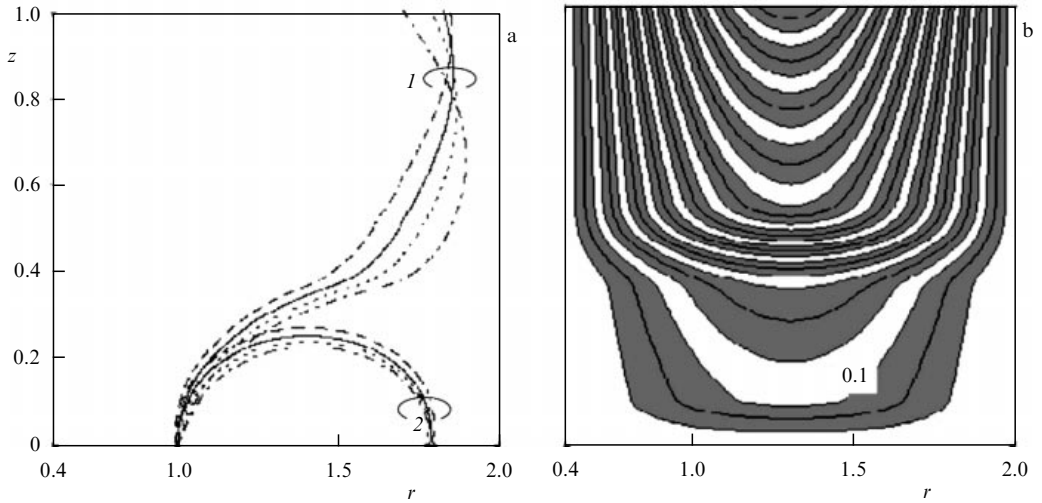

Figure 13. (a) Trajectories of (*1*) heavy ($A = 240$ a.m.u.) and (*2*) light ($A = 150$ a.m.u.) ions for angles $\theta = \pm 45°$ and energies $\varepsilon_0 = 10^{-4}$, 10^{-3}. Field $H_\varphi < 0$. (b) Potential level lines ($-\Pi$) normalized to unity; max $|\Pi| = 0.415$ [38].

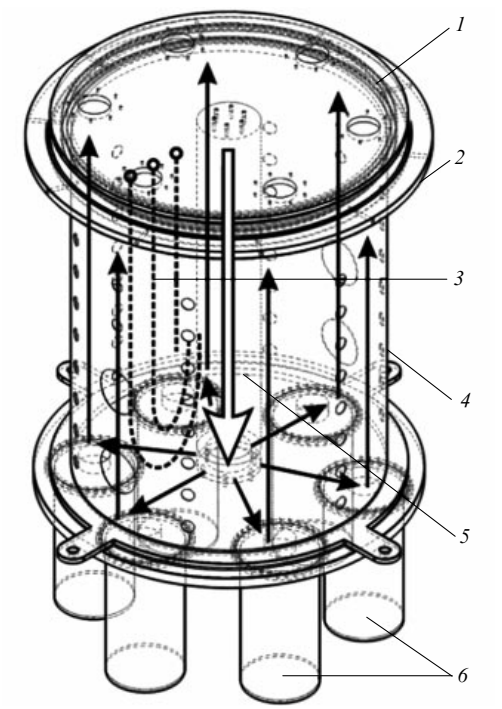

Figure 14. Sketch of a coaxial system for plasma separation of SNF [38]: *1* — insulator, *2* — lateral electrical conductor, *3* — electrodes, *4* — shell, *5* — central electrical conductor, and *6* — plasma source.

6.3 Separation in a curvilinear magnetic field

The ion drift velocity in a curvilinear magnetic field is $v_\mathrm{d} = (v_\parallel^2 + v_\perp^2/2)/(\omega_\mathrm{ci} R)$ [31, p. 44], where R is the radius of curvature of the magnetic lines (the field being generated by a toroid coil). Drift is known to cause a mass-dependent (via the time of flight) deflection of ions from the system's axis in the direction of the binormal toward magnetic lines of force. When all ions in a multicomponent system have equal temperature, the separation effect is insignificant: $\alpha \sim \sqrt{M_\mathrm{i1}/M_\mathrm{i2}}$. It can be expected to enhance if the flux of ions with different longitudinal or transverse energies is directed into a curvilinear magnetic field: $v_\mathrm{d} = [c/(eBR)]\,(2\varepsilon_\parallel + \varepsilon_\perp)$ [128]. Such a method of removal of hot ions from a plasma flux will possibly be employed for the processing of RW and SNF by ICR heating [14, 15, 42] (see Section 7). The separation process is complicated by the fact that centrifugal and gradient drift velocities (terms used in Ref. [99]) denoted by the respective items in the formulas depend on particle charges; this causes electrons and ions to drift in opposite directions and thereby leads to spatial plasma polarization.

It proved possible to purify hydrogen plasma from admixtures by driving the plasma bunch into a sector of the toroidal chamber [129, 130]. These experiments were initiated under the assumption of the action of a drift separation mechanism, but it was discarded as untenable in Ref. [130] to avoid erroneous interpretation of the results (it was estimated that drift motion fails to settle during a bunch passage through the toroidal section).

We are unaware of any studies examining the possibility of a drift-unrelated centrifugal separation effect in the plasma moving in a curvilinear magnetic field. This problem arose from the results of experiments reported by Papernyi and Lebedev [39].

Experiments on plasma separation of the mixtures of chemical elements in a curvilinear magnetic field have recently been conducted at Irkutsk State Technical University [39, 131, 132]. The authors of Ref. [39] declared the intention to evaluate the possibility of using this method for RW reprocessing. They used an axially nonuniform curvilinear magnetic field, i.e., the field with a variable curvature of magnetic lines of force, where its strength decreased from 200 Oe to 20–30 Oe over the distance that spaced the plasma source and the receptacle of the plasma flux. The experimental setup used in Ref. [39] is illustrated in Fig. 15.

The cathode employed in the vacuum-arc discharge (see Fig. 15) was made from an alloy composed of a solid tungsten solution (17%) in iron. The plasma formed in the discharge spread out in the curvilinear magnetic field, and the separation effect was evaluated from the sediment composition on three collectors. One of them was placed in the xz-plane, and the two others were displaced 6 and 10 cm along the y-axis. The last collector was located practically on the diameter of

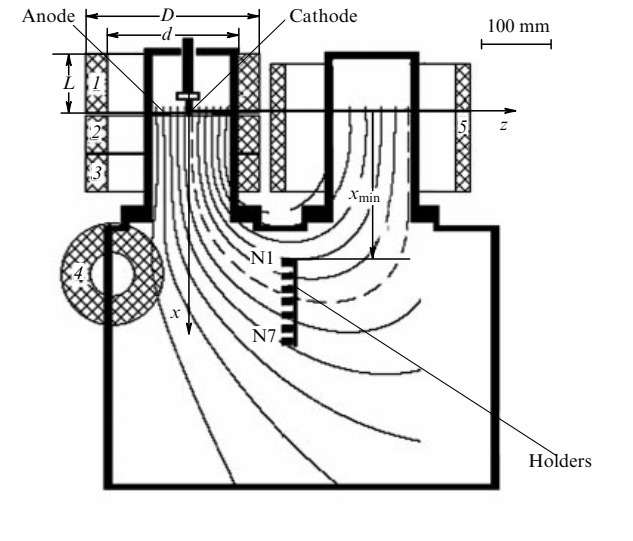

Figure 15. Schematic of experimental setup [39] (top view): *1–5* — solenoids producing magnetic field, N1–N7 — substance collection sites, and x_{min} — distance from plane *yz* to sampling site N1.

the flux cross section deflected from the *xz* plane. The deflection sign, $\pm y$, depended on magnetic field direction. Each collector was designed to receive seven samples. The pulsed-periodic discharge with a repetition rate of 30 Hz was utilized in Ref. [39], in contrast to the stationary one in earlier work by the same authors [131, 132]. The amount of substance sufficient for the analysis of composition accumulated in the samples within 30 min. Sediment composition was determined by electron probe X-ray spectroscopy, which allowed the relative content of constituent components in the samples to be evaluated. Their absolute amounts were not measured.

The study revealed the presence of the radial separation effect with the separation factor $\alpha \approx 8$ computed based on samples No. 2 and No. 4 containing large amounts of substance ($y = -10$).

The authors of Ref. [39] described the observed separation of the W–Fe mixture as the centrifugal separation effect, and attributed the deflection of the plasma flux in the $\pm y$ direction to the influence of the electric drift (on the assumption that the radial electric field is generated in the plasma by centrifugal force).

Reference [39] attracts attention, since it proposes a very simple procedure for the RW and SNF processing. However, the interpretation of the observed separation effect as a centrifugal effect needs to be better substantiated. The centrifugal separation effect in a fully ionized plasma [45] is possible only if it possesses a high enough density ($10^{13} - 10^{14}$ cm^{-3}), because it arises from ion–ion collisions and the time needed for its development must be shorter than the ion time of flight. The fulfillment of these conditions remains to be demonstrated. In fact, the diagnostic methods employed in VAC experiments (see Section 2.2) should be applied.

Interpretations of the above results could be facilitated by the employment of a toroid coil instead of a modular magnetic system (solenoids *1–5* in Fig. 15).

To recall, an attempt was undertaken in the 1950s to find an alternative to gas centrifuges making use of E W Becker's jet nozzle to create curved gas flows [133].

6.4 Separation in moving plasma bunches

The approach proposed in Ref. [40] was based on the results of experiments on the purification of hydrogen plasma bunches from admixtures [134], carried out in the laboratory headed by A I Karchevskii (Kurchatov Institute of Atomic Energy) in the framework of a CNF project in the early 1960s. Plasma bunches had to be purified before their adiabatic compression by an increasing external magnetic field. The plasma formed in the source by electric breakdown over the hydrogen-saturated titanium ring surface with subsequent discharge ($\tau \leqslant 10$ μs) contained carbon, fluoride (from fluoroplastic insulators), and titanium ions, besides protons. The experimental unit had a 5-m long vacuum chamber placed in a solenoid generating a $\leqslant 1$ kOe guiding magnetic field. The plasma source and the mass spectrometer designed as proposed in Ref. [135] were located at opposite ends of the vacuum chamber. The chamber had a glass section equipped with two coils for plasma compression in the mirror trap by a pulsed magnetic field ($R \approx 2$).

A radiointerferometer ($\lambda = 2$ mm) was used to measure plasma density in the source. Its maximum values ($\approx 5 \times 10^{12}$ cm^{-3}) were recorded near the pulsed coils. The plasmoid propagation rate was $(3-5) \times 10^6$ cm s^{-1}. MS measurements (Fig. 16a) revealed that protons concentrated over a flight distance of several meters in the front part of the bunch, while ions of impurities (carbon, fluoride, titanium) went behind. Such spontaneous separation possibly occurred because both protons and admixture ions in the so-called pulsed titanium plasma source used in the study acquired directed energy of the same order of magnitude.

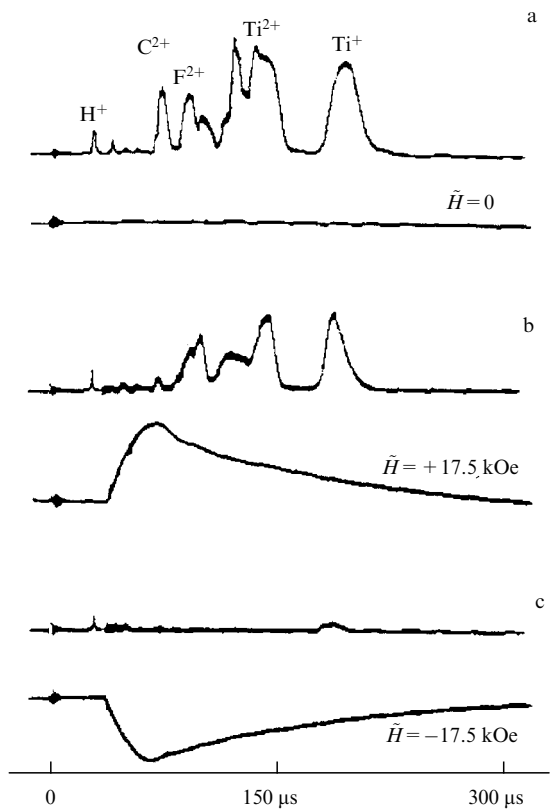

Figure 16. Cutting off admixtures from the hydrogen plasma bunch [40]. MS signal in the case of free propagation of the plasma bunch (a), in the presence of a magnetic barrier ($R \approx 20$) (b), and with a region containing the counterdirected magnetic field (c).

In early experiments with an admixture cut-off, one of the coils designed to compress plasma in the magnetic trap was utilized (thickness 5 cm, mean winding diameter 14 cm). The field in the coil increased for time $\tau \approx 30$ μs, the coil was short-circuited when the current became maximum, and then the magnetic field decayed for 250 μs. The field was created with a controlled delay relative to the plasma source operation time. At the beginning, the magnetic mirror was used to act as the shutter (mirror ratio $R \approx 20$). It allowed confining only ~ 10 eV ions, but not ion fluxes with an energy of ~ 100 eV (Fig. 16b). Admixtures were cut off by the shutter producing the magnetic field counterdirected to a guiding field (Fig. 16c).

Further experiments showed that admixtures can be cut off applying a weaker counterpropagating magnetic field (3–5 kOe), the critical factor being the magnetic configuration in which the force lines of a guiding field intersected the chamber walls. Admixture ions moving along the magnetic field reached the walls, where they recombined, while deposited C and Ti formed the sediment. It was revealed that the energy spectrum broadened with increasing ion mass and doubly-charged ions outran singly-charged ones [40]. Under these experimental conditions, it was impossible to collect titanium totally free from carbon: cutting off the plasmoid tail would allow only a fraction of the titanium containing no carbon admixture to be deposited on the walls.

Thus, future model experiments with other sources of plasma bunches should be focused on the elucidation of the energy characteristics and charge composition of their ions. The above experiments gave evidence of the possibility of cutting off plasmoid fragments.

7. Use of ion cyclotron resonance

7.1 Isotope separation in plasma by the ion cyclotron resonance method

Experiments on 'panoramic' separation of the mixtures of chemical elements by the ICR method have never been reported. This technique was utilized only for isotope separation that required a different study design for obtaining a single isotope, in contrast to the removal of all elements (uranium fission products) as needed for SNF processing. In the former case, a highly uniform magnetic field $\Delta B/B < \Delta M/M$ is employed [85]; in the latter case, the nonuniform field must decrease over the plasma flight path to allow sequential heating at cyclotron frequencies of all ions by a single- or double-frequency HF electric field. At the same time, almost all specific technical issues are similar: from the creation of 'metal' plasma [136] (i.e., conversion of metallic raw materials into the plasma phase) to calculation of the extraction factor of a plasma target component from the plasma stream [77, 78]. Work on ICR isotope separation is briefly reviewed below.

Fundamental experiments on plasma isotope separation (Dawson et al. [85], USA) date back to the mid-1970s. Subsequent studies undertaken by Thompson Ramo Wooldridge, Inc. (TRW) and supported by the United States Department of Energy (DOE) were designed to develop an ICR-based method for the commercial-scale processing of uranium isotopes. However, they were interrupted in the early 1980s. Instead, experiments on the separation of isotopes of stable chemical elements (nickel, indium, lead, and somewhat later palladium) were initiated [137]. They continued until the late 1980s and ended in the successful recovery of the ^{102}Pd isotope from palladium. At the end of the 1990s, the DOE leased the experimental unit to Theragenics Corporation (TGX) for the production of TheraSeed medication showing anti-tumor activity and containing the ^{103}Pd isotope obtained by neutron bombardment of ^{102}Pd. TGX constructed in Oak-Ridge a separate building for the unit with a large superconductor solenoid and put it into operation in the early 2000s.

TGX planned to separate isotopes of various chemical elements on an industrial scale [138]. The work was initially done in the framework of a DOE project (unrelated to medical applications) aimed at developing improved burning out admixtures for commercial nuclear power reactors. Isotopes of gadolinium, dysprosium, and erbium (^{157}Gd, ^{164}Dy, ^{167}Er) were chosen for isotopic enrichment. The experimental results were presented in report [139]. Further work on ^{102}Pd separation took almost a year and was discontinued in 2005. Thereafter (since 2006), TGX switched to a more profitable business (data taken from its annual reports).

Summing up the discussion of research on ICR isotope separation in the USA, where this method is known as the plasma separation process (PSP), it is worthwhile to mention experiments on rubidium isotope separation at the University of California, Los Angeles [140] and ICR recovery of gold from a copper–gold–zinc alloy (77.88% Cu, 17.51 % Au, 4.61 % Zn) by Non-Linear Ion Dynamics LLC, Los Angeles [43]. The maximum separation factor achieved in the latter work carried out with the use of milligram quantities of the substance, was $\alpha \approx 5$. The separation technique fully conformed to the generally accepted one, but the extraction coefficient of gold from the plasma stream proved to be as low as the isotope separation factor (a few percent).

In 1985–1997, experiments on the ICR separation of isotopes were carried out in France with d'Experience de Resonance Ionique Cyclotron (ERIC) (P Louvet and colleagues.) based at the Nuclear Research Centre, Saclay. The installation had a superconducting solenoid ($B \leqslant 3$ T). Calcium, barium, gadolinium, and other elements were chosen for isotope separation [24, 141–145]. The ultimate objective of gadolinium experiments was the development of a commercial-grade technology for ^{157}Gd extraction, because it was generally believed in the 1990s that the utilization of ^{157}Gd-enriched gadolinium as a burning out admixture to the fuel for water–water energetic Reactors (WWER) was commercially more viable than the application of natural gadolinium.

In Russia, ICR separation of isotopes was studied in the laboratory headed by A I Karchevskii (former Kurchatov Institute of Atomic Energy, presently NRC 'Kurchatov Institute') [146–149]. The copper coil solenoid produced a magnetic field not higher than 0.3 T; therefore, the researchers used lithium plasma (to separate ^{6}Li and ^{7}Li). Simultaneously, they developed (based on their own experience and analysis of other experiments) a universal ICR device and the *method of cyclotron ion resonance of isotopes* (MCIRI) — project 0830 of the International Science and Technology Center (ISTC) in Moscow (1999–2000). The superconducting solenoid producing a highly uniform magnetic field $\Delta B/B < 2 \times 10^{-4}$ over a length of 4.7 m in the cylindrical volume with a 0.125-m^2 cross section at $B = 3.3-4.3$ T was designed in the Laboratory of Superconducting Magnetic Systems (NRC 'Kurchatov Institute') headed by V E Keilin.

The extremely high uniformity of the field was deemed necessary to recover the ^{157}Gd isotope ($\Delta M/M \approx 6 \times 10^{-3}$). According to the second condition for selective heating [85], $\omega_{ci}\tau(\Delta M/M) > 1$, where $\tau = L/v_{||}$, the field must be uniform over a length L of several meters. Neither ERIC nor the TGX-leased facilities produced such highly uniform fields, which partly accounts for the low separation factors of gadolinium isotopes obtained in the respective experiments [139, 143]: $\alpha = 2-3$.

Unfortunately, experiments on gadolinium ICR isotope separation could not be continued for lack of financial means for creation of the MCIRI installation. The projected effective output of the unit for the production of 70–80% ^{157}Gd isotope (natural abundance 15.65%) could be 100–200 g/day.

Here are some selected parameters of the superconducting magnetic system (SMS) characterizing the ICR-MCIRI facility: magnet coil length of 6.3 m, conductor (Nb–Ti alloy) length of 53 km, and solenoid mass of 6.4 t. The solenoid is placed inside a 7-m long cryostat having a 'warm' opening 0.9 m in diameter. The SMS mass is ≈ 20 t. These figures give an insight into the magnetic system proposed for RW and SNF processing (see Section 7.2).

There are several review articles providing more or less detailed information about the ICR method for isotope separation [24, 25, 150–153].

7.2 Processing of radioactive waste and spent nuclear fuel by the ion cyclotron resonance method

The first report [14] concerning the ICR method for RW and SNF reprocessing listed a few problems pertinent to plasma technologies, including the separation of groups of elements with similar chemical properties. It appears that the authors meant separation of lanthanides and actinides (see Section 5.2). In a later paper [15], most of the attention was given to processing the SNF from fast neutron reactors. Recycling nuclear fuel implies its depletion in fission products to 1–10% [154] with the use of such technological operations as the removal of the fuel shell in the fuel element, its disintegration into micrometer-sized particles, and degassing the resulting powder by heating and further grinding. The fuel will be injected into the plasma source of the separator in the form of solid submicrometer particles. The plasma source will be an ECR (ultrahigh frequency, UHF) discharge in the magnetic field at an electron cyclotron frequency. Belt type conveyors with interchangeable collectors of SNF fractions will be placed at the exit from the ion ICR-heating zone. An estimate is provided for the SNF flow being separated in a plasma column 1 m in diameter at a plasma (without multiply charged ions) density of 10^{13} cm^{-3}: 150 t per year.

To reach radiation equivalence in the buried processed SNF from fast neutron reactors (in compliance with environmental regulations), the extracted fission products must contain no more than 0.1% of actinides (U, Pu, Am, Np, Cm) [155].

A theoretical analysis of the processing of SNF from fast neutron reactors was undertaken by A V Timofeev [42, 156, 157]. The essence of the approach to nuclear fuel reprocessing consists in selective heating of fission products (nuclear ash, NA) present in an ionized SNF flux and separating them from cold ions of the nuclear fuel (NF). Masses of nuclei in the NA vary in the range of $85 \leqslant A \leqslant 150$ a.m.u. Therefore, the heating area (antenna heating zone) must lie in a decaying external magnetic field to ensure the resonant heating of the ions with the use of a single-frequency HF generator. Figure 17 illustrates the dependence of the magnetic field on the distance:

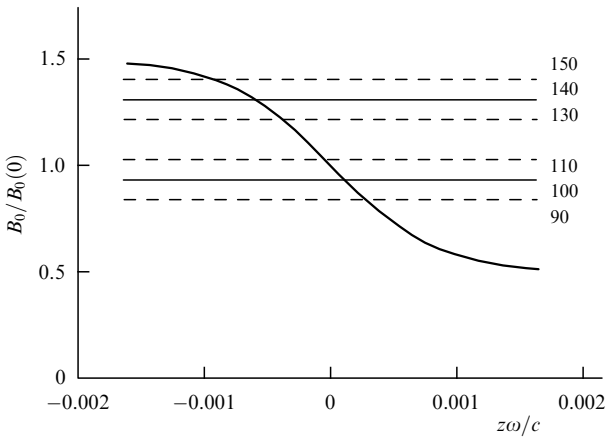

Figure 17. Stationary magnetic field plotted vs the distance along the system's axis [156]. Horizontal lines are resonant values of the magnetic field for ions with the shown atomic number A. Resonance condition in the center of the ICR heating system is supposed to be fulfilled for ions with $A = 107$.

$$B_0(z) = \left(1 - \beta \tanh \frac{z}{L_{B_0}}\right) B_0(0), \quad \beta = 0.5\,.$$

To recall, the inductance antenna of ICR separation devices heating ions is placed inside a metal vacuum chamber, i.e., its conducting elements are between the walls and the plasma column. Calculations of NA ion heating in Ref. [156] were made for an HF field created by a screw antenna, the properties of which the author had described in an earlier paper [158]. A half-wave variant of this antenna was used in the ERIC facility for isotope separation [144].

Here are the parameters of a device for ICR processing of SNF proposed in Ref. [156]: plasma column length of over 4 m, magnetic field at the center of the heating system $B_0(0) \approx 2$ kG (see Fig. 17), initial plasma density $n_0 = 10^{13}$ cm^{-3}, plasma column radius at the entrance to the separator $r_0 = 10$ cm, antenna length $2L_A = 4$ m and radius $r_A = 0.5$ m, and vacuum chamber radius of $2\,r_A$. This variant is applicable when ionized SNF plasma is isothermal and has high enough ion temperature $T_e = T_i = 5$ eV.

Figure 18 shows the computed distribution of ions over transverse velocities at the exit from the ICR heating system with the current in the heating antenna $I_A = 3$ kA. The average NA ion energy totals ≈ 0.4 keV.

Heating NA ions in weak magnetic fields, $B_0(0) = 2$ kG, makes it possible to apply an extraction technique appropriate for the work with radioactive materials. If all heated ions involved in Larmor rotation go beyond the plasma column (Larmor radius of the ions is $\rho_{Li}\,[\text{cm}] = 143\sqrt{W_\perp}\sqrt{A}/(ZH)$, where $W_\perp$[eV] is the ion kinetic energy across the magnetic field, A[a.m.u.] is the ion mass, and H [Oe] is the magnetic field strength), external collectors can be involved.

The external collectors may be either a cylinder encompassing the plasma column or a flat ring with a hole having an area bigger than the plasma column cross section ('longitudinal' and 'transverse' collectors, respectively) [156, 157]. A longitudinal collector must be extended, because heated ions are deposited within the step of their helical trajectory. These

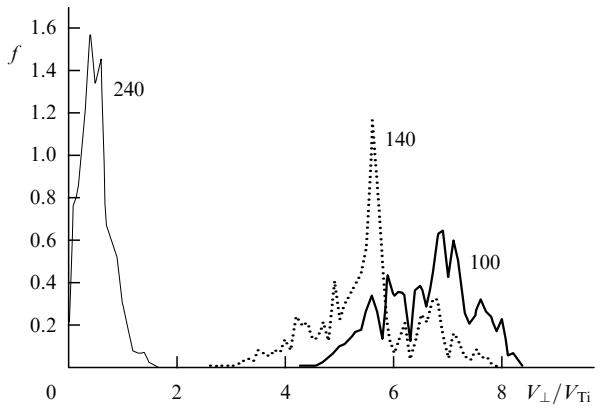

Figure 18. Ion distribution f over transverse velocities at the exit from the ICR heating system [156]. The frequency of the HF field is equal to the cyclotron frequency of ions with $A = 107$ a.m.u. in the center of the ICR heating system ($z = 0$) (see Fig. 17); ion atomic numbers are shown alongside the curves.

devices installed at the exit from the ICR heating zone allow avoiding the use of an additional section with the curved magnetic field, as proposed in Ref. [14], in which heated ions could be extracted as they drift in the direction of the binormal toward magnetic field lines [128]. The application of longitudinal and transverse collectors prevents 'panoramic' separation, since the selectively heated NA components are mixed on them.

What can hamper successful application of this RW and SNF processing technique? The author of Ref. [156] points out a problem associated with single-frequency ion heating in the presence of doubly-charged actinide ions in ionized SNF. These ions are likely to be heated and removed from the flow together with NA ions ($\omega_{ci} = ZeH/(M_i c)$). According to paper [156], a radical solution to this problem lies in double-frequency ion heating, allowing NA ions with mass number $A \approx 120$ a.m.u. that make up a negligible admixture in actinides to be excluded from the heating process (the probability of dividing a nucleus into two equal parts is very low).

A variant of SNF processing with the use of double-frequency ICR heating is considered in Ref. [157]. Isotope separation is possible at a lower magnetic field gradient: $\beta = 0.11$. Cyclotron heating frequencies are $\omega_1 = \omega_{ci}$ ($A = 97$ a.m.u.), and $\omega_2 = \omega_{ci}$ ($A = 143$ a.m.u.). They are calculated for a magnetic field in a cross section with coordinate $z = 0$ (see Fig. 17). The permissible total concentration of multiply charged ions in ionized SNF is $\xi \leqslant 10\%$. This limitation is related to the removal of NA. The author argues that such a concentration still permits operations with multiply charged NA ions to be avoided.

Selective heating and extraction of multiply charged ions encounters even more difficulties, because $\nu_{ii} \propto Z^4$, $\rho_L \propto 1/Z$, etc. (such dependences are, on the contrary, favorable for single-frequency heating, since they are associated with a reduced actinide admixture in nuclear ash). The formation of multiply charged ions in a moving plasma may continue outside the plasma source by virtue of electron thermal conductivity. Because $\xi \propto n_i L$, plasma density should be diminished (and a shorter separator used) to decrease the proportion of multiply charged ions. Lowering the plasma density reduces separator efficiency. The author of Ref. [157] proposed to make up for this reduction by increasing the flow cross section and using wide-band plasma jets.

Qualitative confirmation of certain items in the proposed schemes was obtained in experiments on the ICR separation of isotopes. Indeed, the selectively heated ions leave the plasma column. This observation provided a basis for their selection in experiments on the separation of rubidium isotopes [140] with the use of an external transverse collector [159]. The brief report [140] contains no data on the ^{87}Rb (27.8% in natural rubidium) extraction coefficient. In Ref. [108], the drift of heated ions beyond the initial plasma column boundary was recorded by an annular analyzer of ion energies.

Numerous measurements of plasma flow depletion after extraction of resonant ions were made using the ERIC facility [142, 144]. The results may serve as a guide for addressing the problem of NA extraction from SNF. However, the experimenters exploited a collector system submerged into plasma; therefore, their results cannot be automatically extrapolated to studies with the use of external collectors. The depletion factor was calculated from formula $\beta = [c_w/(1-c_w)]/[c_0/(1-c_0)]$, where c_0 is the initial concentration of the isotope to be recovered, and c_w is its concentration in the waste.

As a rule, $1/\beta < \alpha$, probably for two reasons: not all extractable ions were heated, and not all heated ions were collected. Starting from Ref. [85], a positive retarding potential V_r has been applied to collectors to increase final product enrichment. As a result, weakly heated ions of the isotope of interest are repulsed together with other isotope ions, move into the waste collector, and thereby contribute to a decrease in β.

The only extraction experiment at $V_r = 0$ was conducted with the ^{64}Zn isotope (natural content 48.6%) [42], yielding $\beta \approx 0.26$. What can be the result of SNF processing with such a depletion factor? Let us assume that SNF from a fast neutron reactor contains 20% of NA. Evidently, NA content will be reduced to 5%. Is it worthwhile to apply a negative drawing potential V_d to the collector? Bearing in mind the volt–ampere characteristic of the collector [160], it would hardly change β. In addition, it should be taken into consideration that ERIC experiments were carried out with plasma fluxes that transferred hundreds of milligrams of substance per hour [144].

The ERIC experiments also included concentration measurements of doubly-charged ions in plasma created by the ion source [143, 144] using a miniature mass spectrometer (see Fig. 5 in Ref. [144]) introduced into the vacuum chamber cross section at the distance of ≈ 10 cm from the plasma source. The mass spectrometer was either drawn close to the plasma column ($R \approx 5.5$ cm) or immersed into plasma 1.0–1.5 cm deep to measure the level of doubly-charged ions only in the peripheral region of the ERIC plasma, $\rho_L \ll R$. In most experiments (ionization of Mg, Ca, Zn, Ba, Yb vapors), the proportion of doubly-charged ions $n_i(2+)/n_i \sim 1\%$ [144]. In argon–gadolinium plasma with equal concentrations of Ar and Gd ions (50% each), the proportion of doubly-charged Gd^{2+} ions was 14% [143].

The authors of these studies ruled out the strong effect of multiply charged ions at such concentrations on the isotope separation process. This aspect was also omitted in work on the ICR separation of lithium isotopes, because the ionization potential of a singly-charged lithium ion is 75.6 eV [52, p. 419]. Notice also the favorable situation for palladium isotope

separation due to the second ionization potential equaling 19.4 eV. At the same time, calculations confirmed the possibility of the formation of doubly-charged ions in gadolinium plasma sources [161].

7.3 Particle losses in plasma transport

Particles are lost through ion–electron and ion–ion collisions with frequencies ν_{ie} and ν_{ii} at plasma densities $\geqslant 10^{12}$ cm^{-3}. The quantity $\nu_{ie} = 2 \times 10^{-5} n_i Z_i^2 / T_e^{3/2}$ [31, p. 60] defines ambipolar diffusion. According to estimation [42], the diffusion time is roughly by two orders of magnitude greater than the plasma time of flight through a 3 m long system. Ion–ion collisions may result in additional losses [162]. The quasineutrality of the plasma in the case of radial ion transfer in an open magnetic trap could be maintained due to plasma contact with its conducting and electron-emitting ends. However, this does not happen, and the departure of particles to the walls attributable to ion viscosity is not particularly intense.

Numerical simulation of the separator operation [85, 115] gave evidence of significant radial losses of ions (11–15%) in the $\sim$ 1-m long MCMF device at a plasma density of $\sim 10^{12}$ cm^{-3}. To recall, ion separation by masses occurs in MCMF plasma as they are selectively reflected from centrifugal and magnetic mirrors but not during their passage through the filter; therefore, it is necessary to take into account the mass losses over plasma confinement time in the trap that is longer than the time of flight. This may partially explain the calculated magnitude of losses. Reference [31, p. 402] presents a formula allowing an estimate of the relationship between particle losses through the mirrors ('the product' in reality) and during diffusion across the magnetic field in a purely magnetic mirror: $(R/\rho_{Li})^2 \sqrt{M_i}/m_e$, where R is the chamber radius. The losses calculated using this formula do not exceed 1%.

Ion–ion collisions are an indispensable prerequisite for the work of the MCMF. They must be frequent enough to enable ions to fall into the exit cone [31, p. 400] and leave the trap in the proper direction. The required collision frequency ν_{ii} determines the minimal working plasma density. The relation $\nu_{ii} > \nu_{ie} m_e / M_i$ is important for the choice of other plasma characteristics. The working plasma density must be bounded from above in conformity with the permissible level of losses. Let us consider a prediction of substantial losses to be a result of disregarding space charges associated with ion radial motion [115].

Notice the estimate of MCMF efficiency in Ref. [84]: 10 t/yr at a plasma flow radius of 0.4 m and plasma temperature of 10 eV. In all probability, the particle losses referred to in this section will preclude realization of the project in question.

8. Conclusion

The present review covers all of the published proposals concerning plasma processing of RW and SNF, and makes reference to an outlook on their possible future usage. However, the most known proposal among them (APMF, see Section 3) was viewed unfavorably, extensive works launched in the framework of the project was stopped. Later on, Fetterman and Fisch [19, 20] recognized that APMF is an inefficient system that requires a rarefied plasma to be operated, i.e., a plasma with magnetized ions and electrons unable to create an intense substance flow to be separated. The authors of Refs [19, 20] do not refer to observing the Ohkawa effect [6] underlying the APMF design. We mentioned above indirect confirmation of this effect in Ref. [90] and what can possibly be regarded as its direct evidence (although at the indicator level) in Ref. [96].

The magnetic centrifugal mass filter (MCMF) was proposed as an alternative to the APMF [19, 20]. The mechanism of its action is described in Section 5. It was not the first proposal concerning ion mass separation with a contribution from N J Fisch (PPPL, USA). The theoretical basics of new separation techniques have been considered in articles published during the past decade. The authors of Ref. [163] proposed to separate isotopes by directing a purely ionic flux into an undulator placed in a constant magnetic field, as an alternative to ICR separation of isotopes in plasma, which they considered to be inefficient. This approach implied coordination of ion velocity, the undulator parameters, and the magnetic field strength to create cyclotron resonance conditions for isotope ions passing through the undulator and ensure conversion of longitudinal to transverse energy needed for their separation. Reference [116] describes a contactless high-frequency method for driving the rotation of totally ionized plasma in a plasma centrifuge (Fig. 1 shows modes of plasma rotation during which it comes in contact with the electrodes). The authors of Ref. [116] regard this method as suitable for inducing plasma rotation in MCMF [20]. The contactless method for the induction of rotation of a partially ionized plasma was tested in Ref. [164].

The proposal of an MCMF separator [19, 20] was not based on concrete experimental data. Reference [84], designed to estimate the separation power of an MCMF for a mixture of lanthanides and actinides (a challenge for chemists due to the similar chemical properties of these elements), indicated the acceptable plasma density as being roughly 10^{12} cm^{-3}. Formulas for specific separation powers of the MCMF, Ohkawa filter, and plasma centrifuge, along with their comparison at equal plasma densities and temperatures, were given in Ref [165]. The same article provided an example suggesting that the specific separation powers of the Ohkawa filter are comparable with those of a plasma centrifuge and exceed the MCMF power, in contrast to earlier reports of its low efficiency [19, 20]. In other words, estimates of the productive capacity of the Okhawa filter and MCMF are contradictory.

It may be speculated, keeping in mind Ref. [96] that in future research based at the Kharkiv Institute of Physics and Technology (see Section 4) preference will be given to the Okhawa filter. An independent estimate of its efficiency will possibly be made.

Prospects for plasma-optical separation techniques (see Section 6) are thus far unclear for the lack of experimental information. Specifically, the possibility of using the azimuthator, a key element of POMS-E, remains unknown, because the necessary magnitude of the ion current cannot be set for intense plasma streams (see Section 6.1). In a separator with a potential well it is impossible to set a value of current for ions propagating at suprathermal velocities (see Section 6.2). The centrifugal separation effect was probably apparent in the device with a curvilinear magnetic field (see Section 6.3), but these data are insufficient to regard it as an alternative to the plasma centrifuge.

The proposal to take advantage of ion cyclotron resonance in the plasma for RW and SNF processing (see Section 7) specified the desirable productive capacity of the

device with regard to SNF treatment; namely, it must correspond to the efficiency of an electromagnetic separator with an ion current of 200–300 A [15], i.e., be equivalent to the SNF accumulation rate in WWER-1000. The achievement of such efficiency in on-site reprocessing of spent fuel would allow not storing SNF at all. Plasma parameters in an ICR device needed to come close to attaining this goal are given by the formula for an equivalent ion current in a uranium plasma flux moving with the ion-acoustic speed $I_{\mathrm{eq,i}} \approx 10^{-14} nS(T_{\mathrm{e}} + T_{\mathrm{i}})^{1/2}$ [42]. According to this formula, an equivalent uranium ion current of roughly 100 A creates a plasma stream with a density of 10^{12} cm^{-3}, temperature of 5 eV, and cross section of 10^4 cm^2. Such parameters are probably attainable, but SNF processing can be hampered by the high content of multiply charged ions ($> 10\%$) [42].

It would certainly be easier to make an optimal choice between the RW and SNF processing techniques if waste and spent fuel could be transferred into the plasma phase without the production of multiply charged ions. Experiments to this goal are currently underway [166].

References

1. Prusakov V N, Simonov N F, Trotsenko N M, in *Proc. of the Second United Nations Intern. Conf. on the Peaceful Uses of Atomic Energy* Vol. 17 (Geneva: United Nations, 1958) p. 468
2. Veryatin U D et al. *Atom. Energ.* **31** 375 (1971)
3. Trotsenko N M, in *Izotopy: Svoistva, Poluchenie, Primenenie* (Isotopes: Properties, Production, Application) Vol. 2 (Ed. V Yu Baranov) (Moscow: Fizmatlit, 2005) p. 173
4. Ohkawa T, Miller R L *Phys. Plasmas* **9** 5116 (2002)
5. Litvak A et al., in *Proc. of the 30th European Physical Society Conf. on Controlled Fusion and Plasma Physics, St. Petersburg, Russia, 7–11 July 2003* Vol. 27 (London: ECA, 2003) p. O1.6A
6. Ohkawa T "Plasma mass filter", US Patent No. 6,096,220 (2000)
7. Ohkawa T "Tandem plasma mass filter", US Patent No. 6,235,202 B1 (2001)
8. Cluggish B P et al. *Phys. Plasmas* **12** 057101 (2005)
9. Cairns J B S, in *Proc. of Intern. Conf. on Uranium Isotope Separation, London, 1975* (London: British Nuclear Energy Society, 1975)
10. Belorusov A V et al. *Pis'ma Zh. Tekh. Fiz.* **2** 664 (1976)
11. Belorusov A V et al. *Fiz. Plazmy* **5** 1239 (1979)
12. Vlasov V V et al. *JETP Lett.* **27** 247 (1978); *Pis'ma Zh. Eksp. Teor. Fiz.* **27** 264 (1978)
13. Morozov A I et al., in *Dokl. VII Vserossiiskoi* (*Mezhdunarodnoi*) *Nauchnoi Konf. "Fiziko-Khimicheskie Protsessy pri Selektsii Atomov i Molekul"* (Proc. of the VII All-Russian (Intern.) Scientific Conf. "Physico-Chemical Processes in the Selection of Atoms and Molecules") (Moscow: TsNIIatominform, 2002) p. 148
14. Smirnov V P et al., in *Dokl. IX Vserossiiskoi* (*Mezhdunarodnoi*) *Nauchnoi Konf. "Fiziko-Khimicheskie Protsessy pri Selektsii Atomov i Molekul"* (Proc. of the IX All-Russian (Intern.) Scientific Conf. "Physico-Chemical Processes in the Selection of Atoms and Molecules") (Moscow: TsNIIatominform, 2004) p. 7
15. Zhil'tsov V A et al. *Atom. Energy* **101** 755 (2006); *Atom. Energ.* **101** 302 (2006)
16. Skibenko E I et al., in *Proc. of the 2nd Intern. Conf. Current Problems in Nuclear Physics and Atomic Energy, NPAE-2008, Kyiv, Ukraine, June 9–15, 2008*, p. 657
17. Egorov A M et al. *Vestn. Nats. Tekh. Univ. Khar'kovskii Politekh. Inst.* (41) 78 (2009)
18. Yuferov V B *Voprosy Atom. Nauki Tekh.* (3) 96 (2012)
19. Fetterman A J, Fisch N J, PPPL-4627 Report (Princeton: Princeton Plasma Physics Laboratory, 2011)
20. Fetterman A J , Fisch N J *Phys. Plasmas* **18** 094503 (2011)
21. Krishnan M, Geva M, Hirshfield J L *Phys. Rev. Lett.* **46** 36 (1981)
22. Geva M, Krishnan M, Hirshfield J L *J. Appl. Phys.* **56** 1398 (1984)
23. Lafferty J M (Ed.) *Vacuum Arcs. Theory and Application* (New York: Wiley, 1980); Translated into Russian: *Vakuumnye Dugi. Teoriya i Prilozhenie* (Moscow: Mir, 1982)
24. Louvet P, in *Proc. of the Second Workshop on Separation Phenomena in Liquids and Gases* Vol. 1 (Eds P Louvet, P Noe, Soubbaramayer) (Versailles-Saclay: Univ. Paris-Saclay, 1989) p. 5
25. Grossman M W, Shepp T A *IEEE Trans. Plasma Sci.* **19** 1114 (1991)
26. Ustinov A L, in *Itogi Nauki i Tekhniki. Ser. Fizika Plazmy.* (The Results of Science and Technology. Ser. Plasma Physics) Vol. 12 *Plazmennye Metody Razdeleniya Izotopov* (Plasma Methods of Isotope Separation) (Ed. A I Karchevskii) (Moscow: VINITI, 1991) p. 42
27. Karchevskii A I, Potanin E P, in *Izotopy: Svoistva, Poluchenie, Primenenie* (Isotopes: Properties, Production, Application) Vol. 1 (Ed. V Yu Baranov) (Moscow: Fizmatlit, 2005) p. 326
28. Whichello J V, Evans P J, Simpson S W, in *Proc. of the 4th Workshop on Separation Phenomena in Liquids and Gases* (Ed. C Ying) (Beijing: Tsinghua Univ., 1994) p. 215
29. US DOE Small Business Innovation Research, http://www.sbir.gov/sbirsearch/detail/407517
30. Krishnan M, Prasad R R *J. Appl. Phys.* **57** 49 (1985)
31. Artsimovich L A *Controlled Thermonuclear Reactions* (New York: Gordon and Breach Sci. Publ., 1964); Translated from Russian: *Upravlyaemye Termoyadernye Reaktsii* (Moscow: Fizmatgiz, 1963) p. 428
32. Volosov V I *Plasma Phys. Rep.* **23** 751 (1997); *Fiz. Plazmy* **23** 811 (1997)
33. Volosov V I *Nucl. Fusion* **46** 820 (2006)
34. Artsimovich L A, Lukyanov S Yu *Motion of Charged Particles in Electric and Magnetic Fields* (Moscow: Mir, 1980); Translated from Russian: *Dvizhenie Zaryazhennykh Chastits v Elektricheskikh i Magnitnykh Polyakh* (Moscow: Nauka, 1978) p. 120
35. Bondarenko V G, Kuz'min R N, in *Izotopy: Svoistva, Poluchenie, Primenenie* (Isotopes: Properties, Production, Application) Vol. 1 (Ed. V Yu Baranov) (Moscow: Fizmatlit, 2005) p. 290
36. Morozov A I, Savel'ev V V *Plasma Phys. Rep.* **31** 417 (2005); *Fiz. Plazmy* **31** 458 (2005)
37. Bardakov V M et al. *Izv. Vyssh. Uchebn. Zaved. Yad' Energetika* (2) 123 (2011)
38. Smirnov V P et al. *Plasma Phys. Rep.* **39** 456 (2013); *Fiz. Plazmy* **39** 523 (2013)
39. Papernyi V L, Lebedev N V *Plasma Phys. Rep.* **40** 78 (2014); *Fiz. Plazmy* **40** 90 (2014)
40. Babichev A P, Muromkin Yu A, Potanin E P, in *Dokl. X Mezhdunarod. Nauch. Konf. "Fiziko-Khimicheskie Protessy pri Selektsii Atomov i Molekul"* (Proc. of the X Intern. Scientific Conf. "Physico-Chemical Processes in the Selection of Atoms and Molecules") (Moscow: TsNIIatominform, 2005) p. 124
41. Morozov A I *Vvedenie v Plazmodinamiku* (Introduction to Plasma Dynamics) (Moscow: Fizmatlit, 2008)
42. Timofeev A V *Phys. Usp.* **57** 990 (2014); *Usp. Fiz. Nauk* **184** 1101 (2014)
43. Paskalov G, Wong A, in *Intern. Symp. on Plasma Physics, ISPC 19, Bochum, Germany, 27–31 July 2009* (Bochum: Ruhr-Univ., 2009) Paper 25
44. Slepian J *J. Appl. Phys.* **26** 1283 (1955)
45. Bonnevier B *Ark. Fys.* **33** 255 (1966)
46. Bonnevier B *Plasma Phys.* **13** 763 (1971)
47. Lehnert B *Phys. Scripta* **7** 102 (1973)
48. Shpol'skii E V *Atomic Physics* Vol. 1 (London: Iliffe Books, 1969); Translated from Russian: *Atomnaya Fizika* Vol. 1 (Moscow: Fizmatlit, 1963) p. 83
49. James B W, Simpson S W *Phys. Lett. A* **46** 347 (1974)
50. Korobtsev S V, Rusanov V D *Plazmennaya Tsentrifuga — Plazmokhimicheskii Reaktor Novogo Tipa* (Plazma Centrifuge – Plasma-Chemical Reactor of a New Type) (Moscow: TsNIIatominform, 1988)
51. Korobtsev S V et al. *Sov. Phys. Dokl.* **28** 504 (1983); *Dokl. Akad. Nauk SSSR* **270** 876 (1983)
52. Kikoin I K (Ed.) *Tablitsy Fizicheskikh Velichin: Spravochnik* (Table of Physical Quantities. Reference Book) (Moscow: Atomizdat, 1976) p. 200
53. Wijnakker M M B, Granneman E H A *Z. Naturforsch. A* **35** 883 (1980)
54. Potanin E P, Ustinov A L *Fiz. Plazmy* **10** 1040 (1984)
55. Alfvén H *Rev. Mod. Phys.* **32** 710 (1960)

56. Lai Shu T *Rev. Geophys.* **39** 471 (2001)
57. Ellis R F et al. *Phys. Plasmas* **12** 055704 (2005)
58. Teodorescu C et al. *Phys. Plasmas* **17** 052503 (2010)
59. Ellis R F et al. *Phys. Plasmas* **8** 2057 (2001)
60. Belorusov A V, Karchevskii A I *Prib. Tech. Eksp.* (2) 213 (1977)
61. Belorusov A V et al. *Zh. Tekh. Fiz.* **55** 919 (1985)
62. Belorusov A V et al., in *XVII Intern. Conf. on Phenomena in Ionized Gases, Budapest 8–12 July 1985. Contributed Papers* Vol. 2 (Eds J S Bakos, Z Sorlei) (Budapest: The Conference, 1985) p. 765
63. Muromkin Yu A et al., in *XIX Intern. Conf. on Phenomena in Ionized Gases, Belgrade, 10–14 July 1989. Contributed Papers* Vol. 1 (Belgrade: Univ. of Belgrade, 1989) p. 246
64. Hirshfield J L, Levin L A, Danziger O *IEEE Trans. Plasma Sci.* **17** 695 (1989)
65. Karchevskii A I, Averin V G, Bezmel'nitsyn V N *Sov. Phys. JETP* **31** 605 (1970); Karchevskii A I, Averin V G, Bezmel'nitsyn V N *Zh. Eksp. Teor. Fiz.* **58** 1131 (1970);
66. Babichev A P et al. *Zh. Tekh. Fiz.* **42** 1219 (1972)
67. Ikehata T et al. *Appl. Phys. Lett.* **55** 1289 (1989)
68. Krishnan M, Hirshfield J L *Rev. Sci. Instrum.* **51** 911 (1980)
69. Prasad R R, Krishnan M *J. Appl. Phys.* **61** 113 (1987)
70. Hole M J et al. *Phys. Rev. E* **65** 046409 (2002)
71. Krishnan M *Phys. Fluids* **26** 2676 (1983)
72. Kikoin A K, Kikoin I K *Molecular Physics* (Moscow: Mir, 1978); Translated from Russian: *Molekulyarnaya Fizika* (Moscow: Nauka, 1976) pp. 159, 189
73. Prasad R R, Krishnan M *J. Appl. Phys.* **61** 4464 (1987)
74. Del Bosco E, Dallaqua R S, Simpson S W, in *Proc. of 5th Workshop on Separation Phenomena in Liquids and Gases, Foz do Iguacu, Brasil, 1996* (Eds C Schwab, N A S Rodriges, H G Wood) p. 169
75. Simpson S W, Dallaqua R S, Del Bosco E *J. Phys. D* **29** 1040 (1996)
76. Yue Y, Simpson S W *J. Phys. D* **29** 2866 (1996)
77. Babichev A P et al., in *Dokl. VII Vserossiiskoi* (*Mezhdunarodnoi*) *Nauchnoi Konf. "Fiziko-Khimicheskie Protsessy pri Selektsii Atomov i Molekul"* (Proc. of the VII All-Russian (Intern.) Scientific Conf. "Physico-Chemical Processes in the Selection of Atoms and Molecules") (Moscow: TsNIIatominform, 2002) p. 208
78. Pashkovskii V G, in *Dokl. VII Vserossiiskoi* (*Mezhdunarodnoi*) *Nauchnoi Konf. "Fiziko-Khimicheskie Protsessy pri Selektsii Atomov i Molekul"* (Proc. of the VII All-Russian (Intern.) Scientific Conf. "Physico-Chemical Processes in the Selection of Atoms and Molecules") (Moscow: TsNIIatominform, 2002) p. 214
79. Belorusov A V et al. *Pis'ma Zh. Tekh. Fiz.* **6** 358 (1980)
80. Gorbunova E F, Karchevskii A I, Muromkin Yu A *Fiz. Plazmy* **12** 1087 (1986)
81. Potanin E P, Karchevskii A I, Ustinov A L *Zh. Tekh. Fiz.* **48** 472 (1978)
82. Karchevskii A I, Potanin E P, Sazykin A A *Fiz. Plazmy* **5** 1355 (1979)
83. Belorusov A V et al. *Zh. Tekh. Fiz.* **50** 931 (1980)
84. Gueroult R, Fisch N J *Plasma Sources Sci. Technol.* **23** 035002 (2014)
85. Dawson J M et al. *Phys. Rev. Lett.* **37** 1547 (1976)
86. Abdrashitov G F et al. *Nucl. Fusion* **31** 1275 (1991)
87. Bekhtenev A A, Volosov V I *Zh. Tekh. Fiz.* **48** 1657 (1978)
88. Tsushima A et al. *Phys. Rev. Lett.* **56** 1815 (1986)
89. Lehnert B *Nucl. Fusion* **11** 485 (1971)
90. Shinohara S, Horii S *Jpn. J. Appl. Phys.* **46** 4276 (2007)
91. Boswell R W *Plasma Phys. Control. Fusion* **26** 1147 (1984)
92. Keiter P A, Scime E E, Balkey M M *Phys. Plasmas* **4** 2741 (1997)
93. Light M, Chen F F, Colestock P L *Plasma Sources Sci. Technol.* **11** 273 (2002)
94. Yuferov V B et al. *Voprosy Atom. Nauki Tekh.* (5) 100 (2013)
95. Il'icheva V O et al. *Voprosy Atom. Nauki Tekh.* (4) 112 (2012)
96. Yuferov V B et al. *East Eur. J. Phys.* **1** 96 (2014)
97. Rozhkov A M et al. *JETP Lett.* **10** 46 (1969); *Pis'ma Zh. Eksp. Teor. Fiz.* **10** 71 (1969)
98. Rozhkov A M et al. *Plasma Phys.* **12** 519 (1970)
99. Frank-Kamenetskii D A *Lektsii po Fizike Plazmy* (Lectures on Plasma Physics) (Moscow: Atomizdat, 1964) p. 42
100. Zavoiskii E K *Atom. Energ.* **14** 57 (1963)
101. Dovbnya A N et al. *Voprosy Atom. Nauki Tekh.* (4) 51 (2004)
102. Gabor D *Nature* **160** 89 (1947)
103. Mikhailovskii A B, Tsypin V S *JETP Lett.* **3** 158 (1966); *Pis'ma Zh. Eksp. Teor. Fiz.* **3** 247 (1966)
104. Eliseev Yu N, Rozhkov A M, Stepanov K N *Ukr. Fiz. Zh.* **27** 688 (1982)
105. Rynn N et al. *Phys. Rev. Lett.* **33** 765 (1974)
106. Lominadze D G *Cyclotron Waves in Plasma* (Oxford: Pergamon Press, 1981); Translated from Russian: *Tsiklotronnye Volny v Plazme* (Ed. A B Mikhailovskii) (Tbilisi: METSNIEREBA, 1975) p. 63
107. Schmitt J P M *Phys. Fluids* **21** 1461 (1978)
108. Muromkin Yu A, Pashkovskii V G *Sov. J. Plasma Phys.* **14** 436 (1988); *Fiz. Plazmy* **14** 737 (1988)
109. Kovtun Yu V et al. *Tech. Phys.* **55** 735 (2010); *Zh. Tekh. Fiz.* **80** (5) 143 (2010)
110. Kovtun Yu V et al. *Tech. Phys.* **56** 623 (2011); *Zh. Tekh. Fiz.* **81** (5) 35 (2011)
111. Kovtun Yu V et al. *Ukr. J. Phys.* **58** 450 (2013)
112. Wijnakker M M B, Granneman E H A, Kistemaker J *Z. Naturforsch. A* **34** 672 (1979)
113. Ghosh J et al. *Phys. Plasmas* **13** 022503 (2006)
114. Teodorescu C et al. *Phys. Rev. Lett.* **105** 085003 (2010)
115. Gueroult R, Fisch N J *Phys. Plasmas* **19** 122503 (2012)
116. Fetterman A J, Fisch N J *Plasma Sources Sci. Technol.* **18** 045003 (2009)
117. Bekhtenev A A et al. *Nucl. Fusion* **20** 579 (1980)
118. Boyer K et al., in *Proc. of the Second United Nations Intern. Conf. on the Peaceful Uses of Atomic Energy* Vol. 31 (Geneva: UNITED NATIONS, 1958) p. 319
119. Compant La Fontaine A et al. *J. Phys. D* **31** 847 (1998)
120. Gueroult R et al. *Plasma Sources Sci. Technol.* **25** 035024 (2016)
121. Eliseev V A, Poplavskaya E V *Atom. Energ.* **96** 193 (2004)
122. Morozov A I, Lebedev S V, in *Voprosy Teorii Plazmy* Iss. 8 (Ed. M A Leontovich) (Moscow: Atomizdat, 1974) p. 332
123. Bardakov V M, Kichigin G N, Strokin N A *Tech. Phys. Lett.* **36** 185 (2010); *Pis'ma Zh. Tekh. Fiz.* **36** (4) 75 (2010)
124. Bardakov V M, Ivanov S B, Strokin N A *Phys. Plasmas* **21** 033505 (2014)
125. Bardakov V M et al. *Plasma Sci. Technol.* **17** 862 (2015)
126. Demidenko I I et al. *Zh. Tekh. Fiz.* **34** 1183 (1964)
127. Samokhin A A et al. *Tech. Phys.* **61** 283 (2016); *Zh. Tekh. Fiz.* **86** (2) 127 (2016)
128. Timofeev A V *Plasma Phys. Rep.* **26** 626 (2000); *Fiz. Plazmy* **26** 667 (2000)
129. Safronov B G et al. *Zh. Tekh. Fiz.* **32** 678 (1962)
130. Voitsenya V S et al. *Zh. Tekh. Fiz.* **34** 280 (1964)
131. Papernyi V L, Krasov V I *Tech. Phys. Lett.* **37** 988 (2011); *Pis'ma Zh. Tekh. Fiz.* **37** (11) 53 (2011)
132. Papernyi V L, Krasov V I *Plasma Phys. Rep.* **37** 988 (2011); *Fiz. Plazmy* **37** 1057 (2011)
133. Becker E W, in *Uranium Enrichment* (Ed. S Villani) (Berlin: Springer-Verlag, 1979; Translated into Russian: *Obogashchenie Urana* (Moscow: Energoatomizdat, 1983) p. 233
134. Babichev A P et al., in *Proc. of the Conf. on Plasma Physics and Controlled Nuclear Fusion Research* Vol. 2 (Vienna: IAEA, 1966) p. 191
135. Kalmykov A A *Prib. Tekh. Eksp.* (5) 142 (1963)
136. Romessor T E et al. *IEEE Intern. Conf. Record Abstracts, 1983 IEEE Int. Conf. Plasma Science*, p. 71
137. Mussetto M et al. *IEEE Intern. Conf. Record Abstracts, 1983 IEEE Intern. Conf. Plasma Science*, p. 70
138. Stevenson N R, Bigelow T S, Tarallo F J *J. Rad. Nucl. Chem.* **257** 153 (2003)
139. Grossbeck M L, Renier J-P A, Bigelow T "Development of improved burnable poisons for commercial nuclear power reactors", Final Report on NERI Project Number 99-0074 (Tennessee: Univ. of Tennessee, 2003)
140. Carty J S, Wong A, Rosenthal G, in *4th Intern. Conf. on Isotopes, Cape Town, South Africa. 2002, Final Programme and Abstracts*, p. 36
141. La Fontaine A C, Gil Ch, Louvet P *C.R. Acad. Sci. II* **308** 821 (1989)
142. Louvet P et al., in *Proc. of the 4th Workshop on Separation Phenomena in Liquids and Gases* (Ed. C Ying) (Beijing: Tsinghua Univ., 1994) p. 83

143. Pailloux A, Compant la Fontaine A, Louvet P, in *Proc. of the Sixth Workshop on Separation Phenomena in Liquids and Gases* (Ed. I Yamamoto) (Nagoya: Nagoya Univ., 1998) p. 332
144. La Fontaine A C et al. *J. Phys. D* **31** 847 (1998)
145. La Fontaine A C, Louvet P *Plasma Sources Sci. Technol.* **8** 125 (1999)
146. Karchevskii A I et al., Preprint IAE-5239/7 (Moscow: IAE, 1990)
147. Karchevskii A I et al. *Plasma Phys. Rep.* **19** 214 (1993); *Fiz. Plazmy* **19** 411 (1993)
148. Gorshunov N M et al. *Priklad. Fiz.* (3) 34 (2001)
149. Babichev A P et al. *Plasma Phys. Rep.* **40** 760 (2014); *Fiz. Plazmy* **40** 864 (2014)
150. Muromkin Yu A, in *Itogi Nauki i Tekhniki. Ser. Fizika Plazmy*. (The Results of Science and Technology. Ser. Plasma Physics) Vol. 12 *Plazmennye Metody Razdeleniya Izotopov* (Plasma Methods of Isotope Separation) (Ed. A I Karchevskii) (Moscow: VINITI, 1991) p. 83
151. Karchevskii A I, Muromkin Yu A, in *Izotopy: Svoistva, Poluchenie, Primenenie* (Isotopes: Properties, Production, Application) Vol. 1 (Ed. V Yu Baranov) (Moscow: Fizmatlit, 2005) p. 307
152. Dolgolenko D A, Muromkin Yu A *Phys. Usp.* **52** 345 (2009); *Usp. Fiz. Nauk* **179** 369 (2009)
153. Muromkin Yu A *J. Ener. Power Eng.* **7** 306 (2013)
154. Adamov E O et al. *Voprosy Atom. Nauki Tekh. Ser. Obespechenie Bezopasnosti AES* (4) 5 (2004)
155. Adamov E O et al. *Voprosy Atom. Nauki Tekh. Ser. Obespechenie Bezopasnosti AES* (4) 26 (2004)
156. Timofeev A V *Plasma Phys. Rep.* **33** 890 (2007); *Fiz. Plazmy* **33** 971 (2007)
157. Timofeev A V *Plasma Phys. Rep.* **35** 912 (2009); *Fiz. Plazmy* **35** 989 (2009)
158. Timofeev A V *Plasma Phys. Rep.* **25** 207 (1999); *Fiz. Plazmy* **25** 232 (1999)
159. Wong A Y, Rosenthal G B, US Patent No. 5,981,955 (1999)
160. Dolgolenko D A et al., in *Proc. of the 4th Workshop on Separation Phenomena in Liquids and Gases* (Ed. C Ying) (Beijing: Tsinghua Univ., 1994) p. 93
161. Dolgolenko D A, Karchevskii A I, Potanin E P, in *Dokl. V Vserossiiskoi* (*Mezhdunarodnoi*) *Nauchnoi Konf. "Fiziko-Khimicheskie Protsessy pri Selektsii Atomov i Molekul"* (Proc. of the V All-Russian (Intern.) Scientific Conf. "Physico-Chemical Processes in the Selection of Atoms and Molecules") (Moscow: TsNIIatominform, 2000) p. 130
162. Timofeev A V, Kuyanov A Yu *Plasma Phys. Rep.* **36** 931 (2010); *Fiz. Plazmy* **36** 991 (2010)
163. Rax J-M, Robiche J, Fisch N J *Phys. Plasmas* **14** 043102 (2007)
164. Averin V G et al. *Zh. Tekh. Fiz.* **48** 66 (1978)
165. Fetterman A J, Fisch N J *Phys. Plasmas* **18** 103503 (2011)
166. Amirov R Kh *Trudy Mosk. Fiz.-Tekh. Inst.* **6** (1) 136 (2014)